Unraveling the Neuroprotective Effect of Tinospora Cordifolia in Parkinsonian Mouse Model Through Proteomics Approach.

Hareram Birla
Banaras Hindu University
Chetan Keswani
Banaras Hindu University
Saumitra Sen Singh
Banaras Hindu University
Walia Zahra
Banaras Hindu University
Hagera Dilnashin
Banaras Hindu University
Aaina Singh Rathore
Banaras Hindu University
Richa Singh
Banaras Hindu University
Monika Rajput
Banaras Hindu University
Surya Pratap Singh (suryasinghbhu16@gmail.com)
Banaras Hindu University https://orcid.org/0000-0001-5668-1712

Research article

Keywords: Parkinson's disease, Neuroprotection, Tinospora cordifolia, Proteomics, Label free quantification

Posted Date: January 25th, 2021

DOI: https://doi.org/10.21203/rs.3.rs-151144/v1

Abstract

Background

Stress-induced dopaminergic (DAergic) neuronal death in the midbrain region is the primary cause of Parkinson's disease (PD). Approximately 2% of the global population aged above 65 years is affected with PD. Various factors are responsible for the death of DAergic neurons, among which mitochondrial dysfunction, oxidative stress, misfolded protein aggregation and neuroinflammation are the primary factors. From the discovery of L-dopa, multiple drugs were discovered to improve lifestyle of PD patients, but they failed due to their multiple side effects. *Tinospora cordifolia* (Tc), a medicinal herb has been used in traditional medicines to treat neurodegenerative diseases. In our previous study, the neuroprotective role of Tc against MPTP-intoxicated Parkinsonian mice was reported. Here, we further explore the neuroprotective molecular mechanisms of Tc in Rotenone (ROT) intoxicated mouse model through proteomics approach.

Methods

Mice were pretreated with Tc extract by oral administration, followed by ROT-intoxication (2mg/kg body wt. for 35 days, subcutaneous). Rotarod, catalepsy, footprint and pole tests were carried out at 35th day to observe the neuroprotective effects of Tc on motor impairment caused by ROT in PD mice. Protein from nigrostriatal region of the mid brain was isolated, and label free quantification (LFQ) was carried out to identify differentially expressed protein (DEPs) in control vs. PD and PD vs. treatment group. Bioinformatics analysis of DEPs was carried out to explore the molecular pathway, cellular location, molecular function of proteins.

Results

In this study, we report 800 DEPs in control vs. PD and 133 in PD vs. Treatment group. *In silico* tools clearly demonstrate significant enrichment of biochemical and molecular pathways with DEPs which are known to be important for PD progression, including, mitochondrial gene expression, hypothetical network for drug addiction, PD pathways, TGF-β signaling, Alzheimer's disease, Odorant GPCRs and chemokine signaling pathway.

Conclusion

This study provides a novel insight for the disease progression in PD mouse. More importantly, it demonstrates that Tc exerts the therapeutic effects through the regulation of multiple pathways to protect DAergic neurons.

Background

Global burden of neurological diseases has doubled during 1990 to 2015. Among these, Parkinson's disease (PD) growth was fastest in prevalence and death [1,2]. PD is the second most prevalent

neurodegenerative disease with progressive and continuous death of dopaminergic (DAergic) neurons in the grey matter, following to the decrease in Dopamine (DA) concentration in the striatal region [3–5]. The consequential DA deficiency leads to impaired motor function including tremors, rigidity, bradykinesia and akinesia [6]. The centerpiece of PD management is to execute symptomatic treatment with L-dopa but due to its various side effect like nausea, hallucination, dyskinesia, lower blood pressure, confusion, loss of appetite it has limited efficacy [7].

Lately, scientists have been recommending environmental factors (viz. exposure to pesticides) as the contributory factor to PD onset and progression. Recent studies revealed that Rotenone (ROT), a pesticide which is also an inhibitor of mitochondrial complex-I; when administrated consistently, recapitulated PD's features like reactive oxygen species (ROS) generation, degeneration of the nigrostriatal DAergic system etc. [8–10]. As PD advances, the death of DAergic neurons surges and these neurons don't have potency to regenerate. After investigating the available therapeutics used for the treatment of PD, it seems that they only provide symptomatic relief with serious side effects and affects the quality of life. Therefore, the development of effective therapeutic agents having the ability to protect the neurons and to diminish side effects are much needed. Scientists have been working on natural alternatives which provide efficient neuroprotection, subsequent impending basic pathological conditions [11]. The literature study revealed that several medicinal plants including *Mucuna pruriens, Bacopa monnieri, Withania somnifera, Tinospora cordifolia* (Tc) and their active constituents have neuroprotective effects against neuronal cell death in PD [12–16].

Various studies reported that Tc possesses neuroprotective activity and its co-administration with L-Dopa reduces intra neuronal oxidative stress [17]. Kosaraju et al. (2014) in 6-OHDA model of PD reported that, Tc exhibits significant neuroprotective effects as well as improved levels of dopamine and reduces iron toxicity in rat brain [18]. In our previous study, we demonstrated that Tc has neuroprotective as well as anti-neuroinflammatory activity in mice brain mainly due to inhibition of NF-kB and other proinflammatory molecule such as TNF-α, IL-12, IL-1β, and restoration of Tyrosine hydroxylase levels, a key enzyme in the synthesis of DA [19]. Sharma et al. (2020) reported that butanolic extract of Tc has reversed the glutamate-induced neurodegeneration in hippocampus region of rat brain [20].

Proteomics approach accounts for analysis of total protein content at different levels of organization (cell, tissue and organism) at different development stages [21]. Nowadays proteomic approach has ignited much attention in different facets of genomics and cellular behavior. With the help of proteomics, we can identify novel molecular pathways involved in the progression of PD. By targeting these pathways we can conclude early disease diagnosis, prognosis and to monitor the stage of disease development and recognition of advanced drug targets can be achieved [22–25]. Further we can also improve the reproducibility and performance of the available treatment strategies. Therefore, this study was executed to fulfil the gap between PD pathogenesis and treatment strategies [26]. Our study mainly focused on identification of new molecular targets in PD and the mechanism of action through which Tc reverses the disease progression. In the present study, we used label-free quantification (LFQ) based on LC-MS/MS, due to its high sensitivity, reproducibility and reliability to study the protein expression patterns in the

nigrostriatal region of midbrain of mice [27]. Using this method, quantification of the differentially expressed proteins (DEPs) of control vs. Parkinsonian group, and Parkinsonian vs. Tc group was performed. Our results revealed that the Tc treatment improves the behavioral abnormalities in PD mice and in label free proteome analysis, we tried to report multiple proteins in both groups, which were differentially expressed. From these results, we have selected 20 proteins (Supplementary file 2, Table 1)whose expression were significantly modulated in PD as well as treatment group and performed bioinformatics analysis, gene ontology (GO), functional pathway enrichment analysis along with protein-protein interaction (PPI) network and gene-gene interaction, to investigate the correlation with previously reported protein and gene prominent pathway influenced by Tc for neuroprotective activity. These results may assist to figure out the new therapeutic approaches for prevention and treatment of PD.

Materials And Methods

Plant Extract Preparation

Tc stem was procured from Botanical garden, Institute of Science, Banaras Hindu University, Varanasi, India in month of January 2019. Tc stems were dried for 7-10 days in shade and pulverized with the help of an electric grinder. The dried sample was extracted with ethanol and water solvent at a ratio of 70: 30 (200 gm powder into 1000 mL) at 40 °C for 16 h in Soxhlet apparatus. Consequently, the plant extract was filtered through 0.45 μm filter and the residue was concentrated under reduced pressure using rotary vacuum evaporator. The plant extract are expressed in terms of dry weight [28–30].

Ethical Statement

The care and maintenance of the experimental animals was carried out in strict accordance with the Animal Ethics procedure and guidelines of the Institutional Animal Ethical Committee of the Banaras Hindu University, Varanasi, India (Ref no. BHU/DoZ/IAEC/2018-19/032). All the efforts were made to ease suffering of mice used in the study.

For conducting the experiment male Swiss albino mice (25 ± 5 g) was obtained from the animal facility atInstitute of Medical Science, Banaras HinduUniversity, Varanasi (India). The mice were housed in cleanpolypropylene cages with constant light-dark cycles (12/12 h)prior to the experiment. Until the dosing was completed, mice were supplied with water and standard diet pellets ad libitum. The experimental protocol was established in accordance with the guidelines of the Animal Ethics Committee,Banaras Hindu University, Varanasi, India.

Animal Dosing

Animals were randomly assigned into three groups: Control (vehicle group), Rotenone (2 mg/kg body wt. per day) subcutaneously for 35 days and Rotenone + Tc (200 mg/kg body wt. per day) orally-administered for 7 days, then concurrent administration of Tc (21 days) and ROT-intoxication (35 days) were done similar to that Rotenone group (n = 8/group). In accordance with our previous study, dosing

was administered with minor changes [19,31]. Upon completion of the dosing, behavioral analysis was carried out, and the mice were sacrificed to isolate the brains for the proteome analysis. All the experiments were carried out in triplicate.

Behavioral Analysis

To determine the effect of ROT-intoxication on the motor activity in Parkinsonian mouse model, behavioral parameters including the catalepsy test, rotarod test, pole test, and foot-print assay were performed.

Catalepsy Test

Stiffness in the muscles of mice can be estimated by placing the forelimbs of mice on an elevated bar and the hind limbs on the ground. Catalepsy intensity was measured by recording the time when the mice moves their hind limbs from a wooden platform (3 cm in height) to correct their posture. The was recoded in second and the test was discontinued when the time exceeded 180 sec [32].

Pole Test

Initially, for two consecutive days, the mice were trained. The performance was recorded after the last MPTP injection. Mice were placed head-up on the top of a rod (10 mm in diameter, 52 cm in height, with rough surface). T-turn (time taken to orient downward) and T-descend (the time required for the mouse to step down the rod length) were recorded in second and experiment was discontinued after 300 sec [33].

Rotarod Test

For the rotarod test, each mouse was trained in a rotarod before the experiment for three consecutive days, at a set speed of 15 rpm. The time was recorded till the mouse fall from the rotarod and reading were recorded up to 5 min. For each mouse, the test was repeated five times and the mean time was recorded. The difference in fall time observed between the PD group and the Tc-treated group is an indicator of muscle relaxation [34].

Footprint Assay

In the footprint test, the mice were trained to walk on a white paper for three consecutive days. The length of the stride was calculated by immersing the mouse's forefoot in blank ink and measuring the gap between the steps, from the middle toe (first step) to the heel (second step) on the same side of the body [35]. Foot print assay was conducted thrice for each animal. Stride forepaw length were recorded in cm.

Tissue Collection

After behavioral tests, mice were sacrificed by cervical dislocation
followed by decapitation to ensure minimal pain. The brain of each mouse was isolated and instantly

frozen. Later, the brain was dissected under ice cold conditions to isolate the nigrostriatal tissue from the midbrain and was stored at -80 °C until the further experiments were performed.

Sample Preparation for LFQ Analysis

Protein extraction was done following the previous method of Gupta et. al. (2010) with slight modifications [32]. The brain tissue was thawed, and homogenized using the lysis buffer (RIPA, and protease cocktail inhibitor) and incubated for 90 min on ice. The homogenate was centrifuged at 12,000 rpm at 4 ℃ for 20 min, and the supernatant was collected in a fresh eppendorf tube. The proteins were quantified by Bradford assay and expressed in terms of mg/ml/gm. tissue [36]. Quantitative assessment of the protein samples was performed by SDS-PAGE.

100 µg of the protein sample was taken from each group for digestion. The samples were diluted with 50 mM NH_4HCO_3 protein followed by treatment with 100 mM dithiothreitol (DTT) at 95 ℃ for 1 h. 250 mM iodoacetamide (IDA) was added to the RT in dark and incubated for 45 min. The samples were then digested with Trypsin (Trypsin gold promega, USA) and incubated overnight at RT. The resulting sample was vacuum dried and dissolved in 50 µl of 0.1% formic acid (FA) in water, followed by centrifugation at 10,000 rpm and the supernatant was collected into a separate tube. 10 µL injection volume was used on BEH C18 UPLC column for separation of peptides, the mobile phase contained 0.1% FA in water (buffer A) and 0.1% FA in Acetonitrile (98:2 v/v for 1-30 min, 50:50 v/v for 30-40 min, 20:80 v/v for 40-50 min then 98:2 v/v for the next 30 min), and the flow rate was set at 0.3 ml/min. The glutamate level was examined at a wavelength of 472 nm, and the concentration was determined using a standard curve. Three runs per sample were carried out for LFQ. The separated peptides on the column were directed to Waters Synapt G2 Q-TOF instrument for MS and MS/MS analysis. The raw data was processed by MassLynx 4.1 WATERS. The individual peptides MS/MS spectra were matched to the database sequence on PLGS software (ProteinLynx Global Server Software Scores each protein based on the significance of the protein being identified based on MS pattern and MS/MS pattern matching for each peptide, as well as the coverage), WATERS for protein identification. The instrument used for acquiring Mass Spec Data was connected with Waters Synapt G2 (QTOF). The instrument parameters used for identification were Peptide Mass Tolerance at MS1 level: 50 ppm and Fragment Mass Tolerance at MS2 level: 100 ppm. During processing of the sample cysteine sites were modified to carbamidomethylated cysteine, and the methionine sites being prone to oxidation, was considered as a variable modification to the mass (Figure 6) [37,38].

Bioinformatics Analysis

Gene Ontology and Pathway enrichment analysis

The biological significance of DEGs was investigated using WebGestalt, as it is a free online WEB-based gene set analysis toolkit for functional enrichment analysis in different biological levels. In GO and PATHWAY enrichment analysis, we obtained more valuable knowledge about cellular, molecular and biological processes. A p-value < 0.05 was considered a significant enrichment [39].

Protein-Protein Interaction Networks Analysis

Search tool for the retrieval of interacting genes database (STRING) is a database and web resource for forecasting PPI networks. To investigate the relationship between DEGs, the STRING database was used. Our active interaction source of data was text mining, experiments, database, co-expression, gene fusion and co-occurrence. Minimum required score is set 0.7 (higher confidence). By analyzing the predicted interaction networks, we can propose new directions for future experimental research and come up with cross-species forecasts for systematic interconnecting mapping [40].

Investigation through KEGG Mapper tool and Genemania

KEGG mapper tool is used for cellular or biological interpretation of large-scale data sets like genome or meta genome sequence [41]. It comprises of three different databases, Brite, Pathway and Module which, further contains experimental information from the already published literature and represented in the form of these three different pathways. Bioinformatics tools such as Genemania was used for imaging and visualizing the different interacting networks between different genes [42,43]. The interaction between genes may be physical, correlation, colocalize and genetic interactions. It also provides the information about the interaction with unknown genes from already published literature.

Statistical Analysis.

Statistical analysis of behavioral data was done by one-way analysis of variance (ANOVA) using the Student–Newman–Keuls test by GraphPad Prism 6.0. For gene expression, we applied Student's t-test to unequal variances in order to find the p-value for each gene. The results are expressed as the mean ± SEM. p values < 0.05 were considered statistically significant.

Results

Neurobehavioral Parameters

After ROT injection, stiffness was observed in mice by catalepsy test. The latency in the ROT group tended to increase over time ($p < 0.001$), and the observed data was significantly different from those in the control group, but Tc-treated mice showed a shorter latency time ($p < 0.001$), instead of the ROT-intoxicated group (Fig. 1a). In the pole test, ROT-intoxicated mice showed prolonged T-turn in comparison to control group mice ($p < 0.01$). The T-descend duration in Tc pre-treated mice was significantly reduced ($p < 0.01$) (Figure 1b). Rotarod test was performed to check the balance, grip, and movement adjustment of the mice. Compared to control, ROT-intoxicated group had significantly reduced retention time ($p < 0.001$) on rotarod, and it was observed that mice lost motor coordination and grip strength. Compared to ROT-intoxicated mice, Tc treatment significantly increased retention time on rotarod ($p < 0.01$) (Fig. 1c). Footprint analysis showed differences in average stride length between the control group, ROT group, and Tc-treated group. The stride difference in the ROT-intoxicated group was significantly reduced compared

to the control group ($p < 0.01$), whereas the gait disturbance was significantly improved on Tc treatment ($p < 0.05$) (Fig. 1d).

Comparative Protein Profiling Between control vs. PD and PD vs. Treatment Group

The protein profiling was analyzed through PGLC software (Masslynux 4.1 Water, USA) and compared between control vs. Parkinsonian and Parkinsonian vs. Tc mice group. On the basis of fold change, the significance of differences in protein expression was also categorized. The protein whose fold change value was below (≤0.5) were consider downregulated and those protein whose value was greater than 2.0 fold were considered upregulated (Table 1 and Table 2). The label-free LC-MS/MS results demonstrated that control vs. PD group contained 800 DEPs of which 67 were downregulated (Table 1A) and 101 were upregulated (Table 1B). In PD vs. TC group, 133 DEPs were obtained of which 11 (Table 2A) were downregulated and 13 were upregulated (Table 2B). Besides this, some proteins which were significantly expressed in the PD group were normalized by Tc (fold change between (0.5-2.0)) (Supplementary file 1, Figure 2). From this analysis, we identified 20 proteins whose expression was significantly modulated in ROT-intoxicated Parkinsonian group and was efficiently restored with the treatment of Tc. Some prominent upregulated proteins included Short transient receptor potential channel, glutamate receptor inotropic early endosome antigen 1, Serine/threonine-protein phosphatase 2A, transcription factor A, aryl hydrocarbon receptor nuclear translocator, eukaryotic translation initiation factor 5B, prosaposin receptor GPR37, RAC-alpha serine/threonine-protein kinase and neutrophil cytosol factor 4 (Table 2A). whereas ubiquitin carboxyl-terminal hydrolase, DNA (cytosine-5)-methyltransferase 1, phosphatidylinositol 3,4,5-trisphosphate 5-phosphatase 2, ribosome-releasing factor 2, phospholipase D1, receptor-type tyrosine-protein phosphatase, centromere protein I, mothers against decapentaplegic homolog 7, lysine-specific demethylase 3A, T-lymphoma invasion and metastasis-inducing protein 1 were the prominently downregulated proteins (Table 2B).

Gene Ontology and Functional Pathway Enrichment Analysis

To comprehend the potential functions of DEPs in PD, these DEPs were examined. GO analysis (http://www.geneontology.org) of most significant DEPs based on Biological Process (BP), Molecular Function (MF) and Cellular Component (CC) has been shown in (Figure 4, Supplementary file 2 Tables 2, 3 and 4). This analysis revealed that dopamine metabolic process, catechol-containing compound metabolic process, catecholamine metabolic process, adherens junction assembly, mitochondrial gene expression, phenol-containing compound metabolic process, oligodendrocyte differentiation, adherens junction organization, positive regulation of protein modification by small protein conjugation or removal, response to toxic substance were found to be significantly enriched in BP. Furthermore, NMDA selective glutamate receptor complex, neuron spine, cation channel complex, extrinsic component of plasma membrane, cell-cell junction, cell junction, cell surface, trans-membrane transporter complex, ion channel complex, extrinsic component of membrane were significantly enriched in CC. Moreover, TGF-β receptor, cytoplasmic mediator activity, ligand-gated ion channel activity involved in regulation of presynaptic membrane potential, Ca^{2+}-trans-membrane transporter activity, β-catenin binding, heat shock protein

binding, NMDA glutamate receptor activity, δ-catenin binding, Ca^{2+} channel activity was significantly enriched in MF. The criteria for p-values <0.05 was considered significant for enriched GO analysis. To investigate the enriched pathways associated with PD was performed using software Webgestalt (http://www.webgestalt.org). In this study we analyze various significant pathways through Wikipathway (https://www.wikipathways.org/index.php /WikiPathways) which has been shown in (Table 3). Enriched pathway analysis demonstrated that DEPs were highly involved in PD Pathway (Gpr37), Alzheimer's disease pathway, hypothetical network for drug addiction (Grin2a), mitochondrial gene expression (Tfam), lung fibrosis, TGF-β signaling pathway, Hfe effect on hepcidin production, ESC pluripotency (Smad7) and chemokine signaling pathway (Tiam 1).

In silico Analysis through PPI Network

PPIs play a crucial role in understanding the molecular function of DEPs, responsible for the PD onset. As the outcome, hub genes like AKT1, PARK2, MTOR, TFAM, PINK1, TH, SNCA, PID1, PARK7, LRRK2 and App were found with the highest degrees of connection in the network (Figure 5A). In a constructed network, DEPs connected to each other, generally have analogous functions and can be considered as the functional genes. Gene-gene interaction network was constructed to investigate the interaction of significant proteins in the network (Figure 5B).

Discussion

Discovery of L-dopa was a major step forward in the treatment of PD, but its major drawback was the generation of various side effects. In addition, many combinational drugs were reported to reduce the side effects, but the success rate was very low [44]. Besides, the researchers also focused on other molecular targets as well as the alternative treatment options to improve the lifestyle of PD patients. PD attributed by mitochondrial dysfunctions, impairment of protein degradation, oxidative stress and death of DAergic neurons in SN, but the continuous progression of molecular events leading to cell death remains unclear [45]. Prior to designing any preventive intervention, in-depth knowledge of the molecular mechanisms underlying neurodegeneration in PD is required.

ROT, is a well-known pesticide acting selectively on mitochondrial complex I, causing its inhibition like MPP^+. A growing body of proofs suggest that the insecticide model offers more advantages over different experimental models as it will effectively mimic the behavioral and neuropathological symptoms of the illness through the selective degeneration of DAergic neurons [46,47].

PD have various motor (tremor, slowness of movement, rigidity, falls and dizziness, freezing, postural imbalance) [48] and non-motor symptoms (pain, low blood pressure, fatigue, restless legs, swallowing and saliva control, sleep, skin and sweating, bowel and bladder problems) [49]. Various studies reported that non motor symptoms generally develop at the initial stage of PD progression so that it is not able to differentiate PD patients from others. Zahra et al. (2020) reported the characteristic motor impairment in ROT-intoxicated Parkinsonian mice [31]. To check the behavioral deficit in mice, we performed various

behavioral tests such as catalepsy, rotarod, pole, and footprint, which highlighted severe motor abnormalities in ROT-intoxicated PD mouse model [42–45] (Fig 1). Indistinguishable co-ordinates and deterioration of motor skills were also observed in our result due to ROT toxicity, whereas the behavioral tests demonstrates that Tc improves the neurobehavioral shortfall as compared with previous studies [50].

Various medicinal herbs are used for therapeutic functions since ancient times in India, China, and other Asian countries. Medicinal plants are used to treat various neurodegerative diseases [51] and showed very promising results with minimal side effects. Herbs like *Bacopa monnieri, Withania somnifera, Mucuna pruriens,* Tc*,* are tested for its therapeutic potential against neurodegenerative diseases via redox balancing and immunomodulation activities [18,52,53]. In our previous study, we reported that Tc has neuroprotective role via suppressing oxidative stress as well as neuroinflammation [19].

With the application of proteomic profiling analysis, the quantitative and qualitative analysis of thousands proteins from the tangled mixtures along with the demonstrations of their PTMs could be efficiently performed. Based on our findings, we have identified various new molecules and pathways as alternate treatment approach. Here, we used comparative proteome profiling through LFQ/LC-MS/MS to investigate DEP in nigrostriatal region of mice brain. Out of total 800 DEPs, 101 were upregulated and 76 were downregulated in ROT-intoxicated mice compared to control; whereas, out of total 133 DEPs in Tc-treated mice, 13 were upregulated and 11 were downregulated as compared to ROT. Some proteins which are significantly expressed in PD group were reversed by Tc treatment. On the basis of expression and co-relation with PD marker proteins, we selected 20 proteins (Table 2A, Table 2B). Further *in-silico* analysis suggested that some of DEPs (Smad7, Tfam, Grin2a, Gpr37, and Tiam7) play a key role in PD pathogenesis via regulating different signaling pathways (Table 3) and could be a new therapeutic avenue for neuroprotection.

Smad7 is an inactive record factor in pathogenesis of PD, which is constitutively upregulated in triggered microglia [54]. It leads DAergic neurons towards apoptosis by means of p53 and TGF-β cascade. Interestingly, Pal et al. (2016) indicated that activators of either NF-κB (IL-1β, TNF-α) or STAT-1 (IFN-γ) signaling pathways enhances the expression of Smad7 [54,55]. In the present study, we also found an upregulated expression of Smad7 in PD mice which is in agreement with the results of Uberham et al. (2006) whereas, its expression was downregulated after Tc treatment. Upregulation of Smad7 in triggered microglial cell has possessed threat to the neuroprotective TGF-β1 signaling [55,56]. TGF-β signaling favors cell survival by inactivating Bad (pro-apoptotic protein of the Bcl-2 family) thereby enhancing its phosphorylation through activation of the ERK/MAP kinase pathway. TGF-β1 signaling also suppresses the secondary neuronal damage caused by neuroinflammation [57–59]. Thus, TGF-β/Smad signaling pathway plays a crucial role in neuroprotection. Our results also suggests that Tc potentially suppresses the death of DAergic neurons via downregulation of Smad7 [54] .

Tfam (Mitochondrial Transcription Factor A) is a 25 kDa DNA-binding protein contained in mtDNA. Tfam protects mtDNA from ROS, and mtDNA protects Tfam from Lon protease degradation [60, 61]. Loss of

Tfam expression was found to be linked with degeneration of the DAergic neurons [62], whereas its enhanced expression improves mitochondrial ailment phenotypes via accelerating mtDNA copy variety and delays neurodegeneration [63]. Consequently, Tfam is a good indicator of defects in mitochondrial integrity. In this study, we observed that ROT-intoxication upregulates Tfam expression whereas, its expression was downregulated by Tc pretreatment. Lu et al. (2018) also demonstrated a downregulated Tfam expression in ROT-intoxicated cultured SH-SY5Y [64,65]. Thus, it is suggested that by downregulating Tfam expression, Tc improved the mitochondrial function, which is a major pathogenic hallmark of PD.

Gpr37 is a substrate of the E3 ligase Parkin, and henceforth is also called Parkin-related endothelin-like receptor (Pael-R) [66]. Missense type of mutation in PARKIN causes aggregation of Gpr37 in brain of PD patients [67]. Besides, overexpression of Gpr37 prompts its amassing in totals causes ER stress, and neuronal death [66, 68]. On other hand, it has been proposed that native Gpr37 shows neuroprotective property by binding prosaptide and prosaposin [69]. Interestingly, Lundius et al. (2013) reported that overexpression of Gpr37 was robustly protected against ROT, MPP+ or 6-OHDA-induced cytotoxicity in N2a cells [70]. Furthermore, it has been suggested that Gpr37 regulates oligodendrocyte separation and myelination by means of ERK signaling [71]. However, Tc-treatment to the PD mice suppresses the expression of Gpr37 in ROT-intoxicated mice model. Here, we present that Gpr37 plays a broader role in neuroprotective and glioprotective activity of Tc.

Tiam1 (T lymphoma invasion and metastasis 1) is a Rac-specific GEF (Dbl family member), potentially involved in neurodegenerative diseases (AD and PD). It is a Ras effector molecule, stimulated by the Ca^{2+}-dependent activation of the NMDA receptor (NMDAR) [72]. Tiam1 controls the activation of Rho GTPase and plays an important role in PD by regulating oxidative stress and neuroinflammation [73]. Tiam1 controls neurite extension and DAergic neurons differentiation [74,75] . After exposing hippocampal neurons to amyloid-β peptide, Tiam1 is activated and mobilized to the membrane, which may affect the pathology of AD [76]. In the present study, expression of Tiam1 is downregulated by Tc extract treatment against ROT-intoxication. Interestingly, Smith et al. (2017) also reported that, an elevated expression of Tiam1 contributes to neuronal damage [77]. In contrast, Cajanek et al. (2013) showed, Tiam1 as a positive regulator of DAergic neuron differentiation [74]. Together, these studies indicate that ROT-induced neurotoxic effects are linked with an upregulated expression of Tiam1 and Tc reverts the ROT-induced neurotoxicity via downregulating Tiam1 expression.

Akt, a serine/threonine kinase [also known as protein kinase B (PKB)] is an important molecule necessary for neuronal survival as it plays a major role in phosphorylating its substrates, including GSK3, NF-κB, BAD, and forkhead proteins [78]. Downregulation of Akt signaling are seen in PD [79]. Previous studies suggested that PD-inducing neurotoxins including 6-OHDA and MPP+ decreases the expression of pAkt [80]. Durgadoss et al. (2012) demonstrated the Akt signaling impairment in the MPTP-induced mouse model, showing pAkt levels and loss of Akt kinase activity (Thr308 and Ser473). Similarly, we have also reported a downregulated expression of Akt1 in ROT-induced parkinsonian mice. Growing evidence also suggested the importance of mTOR pathway in autophagy and apoptosis which can lead to neuronal

death, but later it was found that was the inhibition of the Akt phosphorylation, rather than mTOR activation that eventually led to neuronal loss [81]. Raghu et al. (2009) reported, activation of Akt by G1-4A (a polysaccharide from Tc) [82]. In an attempt to unravel the anti-apoptotic action of Tc against ROT-intoxication, our study revealed an increased expression of Akt1, also supported by Salama et al. (2020) [83,84].

The present study showed that Tc significantly reversed ROT-induced downregulation of Grin2A expression and exhibits neuroprotective effect against ROT-induced neurotoxicity. Moreover, downregulation of Grin2A (NR2A, a glutamate ionotropic NR type subunit 2A) expression resulted in Ca^{2+}-mediated neurotoxicity. NRs (N-methyl-D-aspartate or NMDA receptors) play a crucial role in the pathogenesis of neurological disorders [85]. Reduced expression of the NRs was found in the patient's brain with neurodegenerative diseases [86,87]. NRs require proper complex formation between GRIN1 and GRIN2 (A-D) subunits to permit Ca^{2+} influx into the cell [88]. GRIN2A, regulates excitatory neurotransmission in the brain and thus plausibly influence the course of PD. Kong et al. (2015) confirmed that Grin2 is downregulated significantly in PD flies against α-synuclein neurotoxicity [89]. Interestingly, in present study we have documented a downregulated expression of Grin2A in ROT-induced parkinsonian mice, whereas, Tc upregulate the Grin2A expression against ROT-intoxication. Similarly, Simon et al. (2017) and Hamza et al. (2011) also reported Grin2A association with the risk of PD [86, 87]. Downregulation of Grin2A showed lack of binding to Grin1 resulting in reduced NMDAR complex formation. By considering all the aforementioned studies the potential of targeting Grin2A for the therapeutics of PD pathogenesis is confirmed. Tc plays an important role in attenuation of NMDAR-dependent Ca^{2+}-mediated signaling via downregulating Grin2A.

Epigenetic dysregulation have emerged as important component in the PD pathogenesis [92]. Kdm3A is a JmjC (Jumonji) domain-containing lysine (K)-specific demethylase 3A. Kdm3A-mediated demethylation of PGC-1α (Peroxisome proliferator-activated receptor gamma coactivator 1-alpha) causes inhibition of subsequent mitochondrial biogenesis and oxidative metabolism via reduction in PGC-1α and Nrf1/2 binding and Nrf1/2-dependent Tfam expression [93]. Dnmt 1 [DNA (cytosine-5)-methyltransferase 1] an enzyme catalyzing DNA methylation via methylating CpGs on hemimethylated DNA. Hypermethylation of PGC-1α promoter results in the reduction of PGC-1α protein expression. Downregulated PGC-1α exacerbates age-dependent neuroinflammation by enhancing the release of IL6 [94].

Overall, epigenetic methylation of PGC−1α positively regulates initiation and progression of PD. Downregulation of PGC−1α via inhibition of Dnmts-mediated hypermethylation, or Kdm3A-mediated demethylation, play central role in PD pathogenesis by improving mitochondrial dysfunction, oxidative and inflammatory stress. In this study, results have shown the downregulation of Dnmts and Kdm3A gene after Tc treatment compared to ROT-induced parkinsonian mice. Hence, Tc may be a potential therapeutic agent for epigenetically modified targets in PD pathogenesis (Figure 7).

Conclusion

This study explored the neuroprotective effect of Tc in ROT-induced PD mouse model. Besides, we have also tried to explore the underlying mechanism of action in restoring the level of various protein molecules including Akt1, Smad7, Gpr37, Grin2A, Tiam1, Tfam, Dnmt1 and Kdm3a etc. In conclusion, the overall findings of this study provides a new insight that Tc exerts therapeutic effect through the regulation of various signaling pathways by protecting the DAergic neurons and restoring mitochondrial function. However, further studies are needed to explore the bioactive components of Tc that play essential role in regulation of the disease.

Abbreviations

DA: Dopamine

DAergic: Dopaminergic neurons

PD: Parkinson's disease

ROT: Rotenone

LFQ: Label free quantification

DEPs: Differentially expressed proteins

ROS: Reactive oxygen species

DTT: Dithiothreitol

PLGS: ProteinLynx global server software

DEGs: Differentially expressed genes

GO: Gene ontology

KEGG: Kyoto encyclopedia of genes and genomes

PTMs: Post translational modifications

Smad7: Mothers against decapentaplegic homolog 7

Tfam: Mitochondrial transcription factor A

Gpr37: G protein-coupled receptor 37

Tiam1: T-lymphoma invasion and metastasis-inducing 1

Grin2A: Glutamate ionotropic receptor NMDA type subunit 2A

DNMTs: DNA methyltransferases

KDM3A: Lysine demethylase 3A

Declarations

Ethics approval

This work has been approved by the Institutional Animal Ethical Committee (Reg no. BHU/DoZ/IAEC/2018-19/032), BHU, Varanasi, India.

Consent for publication

All authors provide their consent for publication

Availability of data and materials

All data generated or analyzed during this study are included in this article [and its supplementary information files].

Competing interests

The authors declare that they have no competing interests.

Funding

The author(s) received partial financial support from Banaras Hindu University, Varanasi for this research.

Authors' Contributions

HB and SPS conceived, performed and designed experiments. HB, SPS, CK and HD wrote the manuscript. HB, SSS, WZ, ASR, RS processed mice tissue for proteomic analysis and perform behavior study. MR and HB perform bioinformatics analysis. All authors approved the final manuscript.

Acknowledgments

SSS, HB, RS, WZ, ASR, and HD are sincerely thankful to ICMR, DBT, CSIR, and BHU, India, for their respective fellowship. The authors are also thankful to the head of the Department of Biochemistry, Institute of science, BHU, for providing the basic departmental facility.

References

1. Ray Dorsey E, Elbaz A, Nichols E, Abd-Allah F, Abdelalim A, Adsuar JC, et al. Global, regional, and national burden of Parkinson's disease, 1990–2016: a systematic analysis for the Global Burden of Disease Study 2016. Lancet Neurol. 2018;

2. Feigin VL, Nichols E, Alam T, Bannick MS, Beghi E, Blake N, et al. Global, regional, and national burden of neurological disorders, 1990–2016: a systematic analysis for the Global Burden of Disease Study 2016. Lancet Neurol. 2019;
3. de Lau LM, Breteler MM. Epidemiology of Parkinson's disease. Lancet Neurol. 2006.
4. Tysnes OB, Storstein A. Epidemiology of Parkinson's disease. J. Neural Transm. 2017.
5. Zhang ZN, Zhang JS, Xiang J, Yu ZH, Zhang W, Cai M, et al. Subcutaneous rotenone rat model of Parkinson's disease: Dose exploration study. Brain Res. 2017;
6. Sulzer D, Surmeier DJ. Neuronal vulnerability, pathogenesis, and Parkinson's disease. Mov. Disord. 2013.
7. Cotzias GC, Papavasiliou PS, Gellene R. Modification of Parkinsonism — Chronic Treatment with L-Dopa. N Engl J Med. 1969;
8. Tanner CM, Kame F, Ross GW, Hoppin JA, Goldman SM, Korell M, et al. Rotenone, paraquat, and Parkinson's disease. Environ Health Perspect. 2011;
9. El-Sayed EK, Ahmed AAE, Morsy EME, Nofal S. Neuroprotective effect of agmatine (decarboxylated l-arginine) against oxidative stress and neuroinflammation in rotenone model of Parkinson's disease. Hum Exp Toxicol. 2018;
10. Bordt EA, Clerc P, Roelofs BA, Saladino AJ, Tretter L, Adam-Vizi V, et al. The Putative Drp1 Inhibitor mdivi-1 Is a Reversible Mitochondrial Complex I Inhibitor that Modulates Reactive Oxygen Species. Dev Cell. 2017;
11. Salamon A, Zádori D, Szpisjak L, Klivényi P, Vécsei L. Neuroprotection in Parkinson's disease: facts and hopes. J. Neural Transm. 2020.
12. Rai SN, Birla H, Singh SS, Zahra W, Patil RR, Jadhav JP, et al. Mucuna pruriens protects against MPTP intoxicated neuroinflammation in Parkinson's disease through NF-κB/pAKT signaling pathways. Front Aging Neurosci. 2017;9.
13. Birla H, Keswani C, Rai SN, Singh SS, Zahra W, Dilnashin H, et al. Neuroprotective effects of Withania somnifera in BPA induced-cognitive dysfunction and oxidative stress in mice. Behav Brain Funct. 2019;15.
14. Jyoti A, Sharma D. Neuroprotective role of Bacopa monniera extract against aluminium-induced oxidative stress in the hippocampus of rat brain. Neurotoxicology. 2006;
15. Cummings J, Lee G, Mortsdorf T, Ritter A, Zhong K. Alzheimer's disease drug development pipeline: 2017. Alzheimer's Dement. Transl. Res. Clin. Interv. 2017.
16. Esposito E, Cuzzocrea S. New Therapeutic Strategy for Parkinsons and Alzheimers Disease. Curr Med Chem. 2010;
17. Sharma A, Bajaj P, Bhandari A, Kaur G. From ayurvedic folk medicine to preclinical neurotherapeutic role of a miraculous herb, Tinospora cordifolia. Neurochem Int. 2020;
18. Kosaraju J, Chinni S, Roy PD, Kannan E, Antony AS, Kumar MNS. Neuroprotective effect of Tinospora cordifolia ethanol extract on 6-hydroxy dopamine induced Parkinsonism. Indian J Pharmacol. 2014;

19. Birla H, Rai SN, Singh S Sen, Zahra W, Rawat A, Tiwari N, et al. Tinospora cordifolia Suppresses Neuroinflammation in Parkinsonian Mouse Model. NeuroMolecular Med. 2019;
20. Sharma A, Kalotra S, Bajaj P, Singh H, Kaur G. Butanol Extract of Tinospora cordifolia Ameliorates Cognitive Deficits Associated with Glutamate-Induced Excitotoxicity: A Mechanistic Study Using Hippocampal Neurons. NeuroMolecular Med. 2020;
21. Srivastava G, Singh K, Tiwari MN, Singh MP. Proteomics in Parkinsons disease: Current trends, translational snags and future possibilities. Expert Rev. Proteomics. 2010.
22. Conti A, Alessio M. Proteomics for Cerebrospinal Fluid Biomarker Identification in Parkinsons Disease: Methods and Critical Aspects. AIMS Med Sci. 2015;
23. Pienaar IS, Dexter DT, Burkhard PR. Mitochondrial proteomics as a selective tool for unraveling Parkinsons disease pathogenesis. Expert Rev. Proteomics. 2010.
24. Kalra H, Adda CG, Liem M, Ang CS, Mechler A, Simpson RJ, et al. Comparative proteomics evaluation of plasma exosome isolation techniques and assessment of the stability of exosomes in normal human blood plasma. Proteomics. 2013;
25. Bantscheff M, Scholten A, Heck AJR. Revealing promiscuous drug-target interactions by chemical proteomics. Drug Discov. Today. 2009.
26. Sleno L, Emili A. Proteomic methods for drug target discovery. Curr. Opin. Chem. Biol. 2008.
27. Megger DA, Bracht T, Meyer HE, Sitek B. Label-free quantification in clinical proteomics. Biochim. Biophys. Acta - Proteins Proteomics. 2013.
28. Alara OR, Abdurahman NH, Ukaegbu CI, Kabbashi NA. Extraction and characterization of bioactive compounds in Vernonia amygdalina leaf ethanolic extract comparing Soxhlet and microwave-assisted extraction techniques . J Taibah Univ Sci. 2019;
29. Prince PSM, Menon VP. Antioxidant action of Tinospora cordifolia root extract in alloxan diabetic rats. Phyther Res. 2001;
30. Ali H, Dixit S. Extraction optimization of Tinospora cordifolia and assessment of the anticancer activity of its alkaloid palmatine. Sci World J. 2013;
31. Zahra W, Rai SN, Birla H, Singh SS, Rathore AS, Dilnashin H, et al. Neuroprotection of rotenone-induced parkinsonism by ursolic acid in pd mouse model. CNS Neurol Disord - Drug Targets. 2020;19.
32. Singh SS, Rai SN, Birla H, Zahra W, Rathore AS, Dilnashin H, et al. Neuroprotective Effect of Chlorogenic Acid on Mitochondrial Dysfunction-Mediated Apoptotic Death of da Neurons in a Parkinsonian Mouse Model. Oxid Med Cell Longev. 2020;2020.
33. Meredith GE, Kang UJ. Behavioral models of Parkinsons disease in rodents: A new look at an old problem. Mov. Disord. 2006.
34. Gupta SP, Patel S, Yadav S, Singh AK, Singh S, Singh MP. Involvement of nitric oxide in maneb- and paraquat-induced Parkinson’s disease phenotype in mouse: Is there any link with lipid peroxidation? Neurochem Res. 2010;

35. Tillerson JL, Caudle WM, Reverón ME, Miller GW. Exercise induces behavioral recovery and attenuates neurochemical deficits in rodent models of Parkinson's disease. Neuroscience. 2003;
36. Bradford MM. A rapid and sensitive method for the quantitation of microgram quantities of protein utilizing the principle of protein-dye binding. Anal Biochem. 1976;
37. Clough T, Key M, Ott I, Ragg S, Schadow G, Vitek O. Protein quantification in label-free LC-MS experiments. J Proteome Res. 2009;
38. Shalit T, Elinger D, Savidor A, Gabashvili A, Levin Y. MS1-based label-free proteomics using a quadrupole orbitrap mass spectrometer. J Proteome Res. 2015;
39. Rajput M, Kumar M, Kumari M, Bhattacharjee A, Awasthi AA. Identification of key genes and construction of regulatory network for the progression of cervical cancer. Gene Reports. 2020;
40. Kangueane P. Protein-protein interactions. Protein-Protein Interact. 2011.
41. Kanehisa M, Sato Y. KEGG Mapper for inferring cellular functions from protein sequences. Protein Sci. 2020;
42. Vlasblom J, Zuberi K, Rodriguez H, Arnold R, Gagarinova A, Deineko V, et al. Novel function discovery with GeneMANIA: A new integrated resource for gene function prediction in Escherichia coli. Bioinformatics. 2015;
43. Warde-Farley D, Donaldson SL, Comes O, Zuberi K, Badrawi R, Chao P, et al. The GeneMANIA prediction server: Biological network integration for gene prioritization and predicting gene function. Nucleic Acids Res. 2010;
44. Ellis JM, Fell MJ. Current approaches to the treatment of Parkinson's Disease. Bioorganic Med. Chem. Lett. 2017.
45. Garcia-Arencibia M, Garcia C, Fernandez-Ruiz J. Cannabinoids and Parkinsons Disease. CNS Neurol Disord - Drug Targets. 2012;
46. Johnson ME, Bobrovskaya L. An update on the rotenone models of Parkinson's disease: Their ability to reproduce the features of clinical disease and model gene-environment interactions. Neurotoxicology. 2015.
47. Schapira AHV, Cooper JM, Dexter D, Clark JB, Jenner P, Marsden CD. Mitochondrial Complex I Deficiency in Parkinson's Disease. J Neurochem. 1990;
48. Williams-Gray CH, Worth PF. Parkinson's disease. Med. (United Kingdom). 2020.
49. Schapira AHV, Chaudhuri KR, Jenner P. Non-motor features of Parkinson disease. Nat. Rev. Neurosci. 2017.
50. Birla H, Rai SN, Singh SS, Zahra W, Rawat A, Tiwari N, et al. Tinospora cordifolia Suppresses Neuroinflammation in Parkinsonian Mouse Model. NeuroMolecular Med. 2019;21.
51. Basnyat S, Kolasinski SL. Ayurvedic medicine for rheumatoid arthritis. Curr. Rheumatol. Rep. 2014.
52. B. K, D.E. G, J. H, K.A. N. Plant metal chaperones: A novel perspective in dementia therapy. Amyloid. 2009;

53. Sharma A, Kaur G. Tinospora cordifolia as a potential neuroregenerative candidate against glutamate induced excitotoxicity: An in vitro perspective 11 Medical and Health Sciences 1109 Neurosciences. BMC Complement Altern Med. 2018;
54. Pal R, Tiwari PC, Nath R, Pant KK. Role of neuroinflammation and latent transcription factors in pathogenesis of Parkinson's disease. Neurol. Res. 2016.
55. Koefer R, Streit WJ, Toyka K V., Kreutzberg GW, Hartung HP. Transforming growth factor-β1: A lesion-associated cytokine of the nervous system. Int J Dev Neurosci. 1995;
56. Ueberham U, Ueberham E, Gruschka H, Arendt T. Altered subcellular location of phosphorylated Smads in Alzheimer's disease. Eur J Neurosci. 2006;
57. Doyle KP, Cekanaviciute E, Mamer LE, Buckwalter MS. TGFβ signaling in the brain increases with aging and signals to astrocytes and innate immune cells in the weeks after stroke. J Neuroinflammation. 2010;
58. Dobolyi A, Vincze C, Pál G, Lovas G. The neuroprotective functions of transforming growth factor beta proteins. Int. J. Mol. Sci. 2012.
59. Krieglstein K, Henheik P, Farkas L, Jaszai J, Galter D, Krohn K, et al. Glial cell line-derived neurotrophic factor requires transforming growth factor-β for exerting its full neurotrophic potential on peripheral and CNS neurons. J Neurosci. 1998;
60. Lu B, Lee J, Nie X, Li M, Morozov YI, Venkatesh S, et al. Phosphorylation of Human TFAM in Mitochondria Impairs DNA Binding and Promotes Degradation by the AAA+ Lon Protease. Mol Cell. 2013;
61. Larsson NG, Wang J, Wilhelmsson H, Oldfors A, Rustin P, Lewandoski M, et al. Mitochondrial transcription factor A is necessary for mtDNA maintenance and embryogenesis in mice. Nat Genet. 1998;
62. Ekstrand MI, Terzioglu M, Galter D, Zhu S, Hofstetter C, Lindqvist E, et al. Progressive parkinsonism in mice with respiratory-chain-deficient dopamine neurons. Proc Natl Acad Sci U S A. 2007;
63. Nishiyama S, Shitara H, Nakada K, Ono T, Sato A, Suzuki H, et al. Over-expression of Tfam improves the mitochondrial disease phenotypes in a mouse model system. Biochem Biophys Res Commun. 2010;
64. Lu J, Chen S, Shen M, He Q, Zhang Y, Shi Y, et al. Mitochondrial regulation by pyrroloquinoline quinone prevents rotenone-induced neurotoxicity in Parkinson's disease models. Neurosci Lett. 2018;
65. Cheng Q, Chen J, Guo H, Lu J li, Zhou J, Guo X yu, et al. Pyrroloquinoline quinone promotes mitochondrial biogenesis in rotenone-induced Parkinson's disease model via AMPK activation. Acta Pharmacol Sin. 2020;
66. Imai Y, Soda M, Inoue H, Hattori N, Mizuno Y, Takahashi R. An unfolded putative transmembrane polypeptide, which can lead to endoplasmic reticulum stress, is a substrate of Parkin. Cell. 2001;
67. Obeso JA, Rodriguez-Oroz MC, Goetz CG, Marin C, Kordower JH, Rodriguez M, et al. Missing pieces in the Parkinson's disease puzzle. Nat. Med. 2010.

68. Marazziti D, Di Pietro C, Golini E, Mandillo S, Matteoni R, Tocchini-Valentini GP. Induction of macroautophagy by overexpression of the Parkinson's disease-associated GPR37 receptor. FASEB J. 2009;
69. Meyer RC, Giddens MM, Schaefer SA, Hall RA. GPR37 and GPR37L1 are receptors for the neuroprotective and glioprotective factors prosaptide and prosaposin. Proc Natl Acad Sci U S A. 2013;
70. Lundius EG, Stroth N, Vukojevič V, Terenius L, Svenningsson P. Functional GPR37 trafficking protects against toxicity induced by 6-OHDA, MPP+ or rotenone in a catecholaminergic cell line. J Neurochem. 2013;
71. Yang HJ, Vainshtein A, Maik-Rachline G, Peles E. G protein-coupled receptor 37 is a negative regulator of oligodendrocyte differentiation and myelination. Nat Commun. 2016;
72. Tolias KF, Bikoff JB, Burette A, Paradis S, Harrar D, Tavazoie S, et al. The Rac1-GEF Tiam1 couples the NMDA receptor to the activity-dependent development of dendritic arbors and spines. Neuron. 2005;
73. Choi DH, Cristóvão AC, Guhathakurta S, Lee J, Joh TH, Beal MF, et al. NADPH oxidase 1-mediated oxidative stress leads to dopamine neuron death in Parkinson's disease. Antioxidants Redox Signal. 2012;
74. Cajanek L, Ganji RS, Henriques-Oliveira C, Theofilopoulos S, Konik P, Bryja V, et al. Tiam1 Regulates the Wnt/Dvl/Rac1 Signaling Pathway and the Differentiation of Midbrain Dopaminergic Neurons. Mol Cell Biol. 2013;
75. Shirazi Fard S, Kele J, Vilar M, Paratcha G, Ledda F. Tiam1 as a signaling mediator of Nerve Growth Factor-dependent neurite outgrowth. PLoS One. 2010;
76. Ma QL, Yang F, Calon F, Ubeda OJ, Hansen JE, Weisbart RH, et al. p21-activated kinase-aberrant activation and translocation in Alzheimer disease pathogenesis. J Biol Chem. 2008;
77. Smith KR, Rajgor D, Hanley JG. Differential regulation of the Rac1 GTPase–activating protein (GAP) BCR during oxygen/glucose deprivation in hippocampal and cortical neurons. J Biol Chem. 2017;
78. Rai SN, Dilnashin H, Birla H, Singh SS, Zahra W, Rathore AS, et al. The Role of PI3K/Akt and ERK in Neurodegenerative Disorders. Neurotox Res. 2019;35.
79. Emamian ES. AKT/GSK3 signaling pathway and schizophrenia. Front. Mol. Neurosci. 2012.
80. Wang C, Ko HS, Thomas B, Tsang F, Chew KCM, Tay SP, et al. Stress-induced alterations in parkin solubility promote parkin aggregation and compromise parkin's protective function. Hum Mol Genet. 2005;
81. Machado-Vieira R, Zanetti M V., Teixeira AL, Uno M, Valiengo LL, Soeiro-de-Souza MG, et al. Decreased AKT1/mTOR pathway mRNA expression in short-term bipolar disorder. Eur Neuropsychopharmacol. 2015;
82. Raghu R, Sharma D, Ramakrishnan R, Khanam S, Chintalwar GJ, Sainis KB. Molecular events in the activation of B cells and macrophages by a non-microbial TLR4 agonist, G1-4A from Tinospora cordifolia. Immunol Lett. 2009;

83. Salama RM, Abdel-Latif GA, Abbas SS, El Magdoub HM, Schaalan MF. Neuroprotective effect of crocin against rotenone-induced Parkinson's disease in rats: Interplay between PI3K/Akt/mTOR signaling pathway and enhanced expression of miRNA-7 and miRNA-221. Neuropharmacology. 2020;
84. Wang C, Cai X, Hu W, Li Z, Kong F, Chen X, et al. Investigation of the neuroprotective effects of crocin via antioxidant activities in HT22 cells and in mice with Alzheimer's disease. Int J Mol Med. 2019;
85. Waxman EA, Lynch DR. N-methyl-D-aspartate receptor subtypes: Multiple roles in excitotoxicity and neurological disease. Neuroscientist. 2005.
86. Mishizen-Eberz AJ, Rissman RA, Carter TL, Ikonomovic MD, Wolfe BB, Armstrong DM. Biochemical and molecular studies of NMDA receptor subunits NR1/2A/2B in hippocampal subregions throughout progression of Alzheimer's disease pathology. Neurobiol Dis. 2004;
87. Meoni P, Bunnemann BH, Kingsbury AE, Trist DG, Bowery NG. NMDA NR1 subunit mRNA and glutamate NMDA-sensitive binding are differentially affected in the striatum and pre-frontal cortex of Parkinson's disease patients. Neuropharmacology. 1999;
88. Prickett TD, Zerlanko BJ, Hill VK, Gartner JJ, Qutob N, Jiang J, et al. Somatic mutation of GRIN2A in malignant melanoma results in loss of tumor suppressor activity via aberrant NMDAR complex formation. J Invest Dermatol. 2014;
89. Kong Y, Liang X, Liu L, Zhang D, Wan C, Gan Z, et al. High throughput sequencing identifies MicroRNAs mediating α-synuclein toxicity by targeting neuroactive-ligand receptor interaction pathway in early stage of Drosophila Parkinson's disease model. PLoS One. 2015;
90. Hamza TH, Chen H, Hill-Burns EM, Rhodes SL, Montimurro J, Kay DM, et al. Genome-wide gene-environment study identifies glutamate receptor gene grin2a as a parkinson's disease modifier gene via interaction with coffee. PLoS Genet. 2011;
91. Simon DK, Wu C, Tilley BC, Lohmann K, Klein C, Payami H, et al. Caffeine, creatine, GRIN2A and Parkinson's disease progression. J Neurol Sci. 2017;
92. Habibi E, Masoudi-Nejad A, Abdolmaleky HM, Haggarty SJ. Emerging roles of epigenetic mechanisms in Parkinson's disease. Funct. Integr. Genomics. 2011.
93. Qian X, Li X, Shi Z, Bai X, Xia Y, Zheng Y, et al. KDM3A Senses Oxygen Availability to Regulate PGC-1α-Mediated Mitochondrial Biogenesis. Mol Cell. 2019;
94. Su X, Chu Y, Kordower JH, Li B, Cao H, Huang L, et al. PGC-1α promoter methylation in Parkinson's disease. PLoS One. 2015;

Tables

Table 1A: list of down regulated protein in control vs. PD group.

Accession	Description	Gene	Score	Fold change	P values
P40630	Transcription factor A, mitochondrial	Tfam	13.77	0.033708673	0.00
Q60I26	ALS2 C-terminal-like protein	Als2cl	34.84	0.103312182	0
Q7M6Z4	Kinesin-like protein KIF27	Kif27	77.06	0.114177608	0
Q9D8U2	Transmembrane protein 41A	Tmem41a	48.37	0.155672628	0
Q8VC28	Aldo-keto reductase family 1 member C13	Akr1c13	8.74	0.170332992	0
Q3TD16	Protein RUBCNL-like	Rubcnl	6.94	0.173773943	0.02
Q9D4D7	Cell cycle control protein 50C	Tmem30c	111.69	0.177284407	0
P28481	Collagen alpha-1(II) chain	Col2a1	26.09	0.184519513	0
Q8K4P0	pre-mRNA 3' end processing protein WDR33	Wdr33	33.73	0.218711891	0
Q9CXJ4	ATP-binding cassette sub-family B member 8, mitochondrial	Abcb8	31.47	0.22090998	0
Q9D824	Pre-mRNA 3'-end-processing factor FIP1	Fip1l1	61.28	0.236927745	0
D7PDD4	Megakaryocyte and platelet inhibitory receptor G6b	Mpig6b	15.59	0.244143291	0.03
Q3V0B4	Cilia- and flagella-associated protein 65	Cfap65	46.43	0.24659697	0.02
Q3UZ18	Little elongation complex subunit 2	Ice2	62.94	0.249075308	0.08
Q3UFQ8	Capping protein, Arp2/3 and myosin-I linker protein 3	Carmil3	100.97	0.254106958	0.02
Q6VGS5	Protein Daple	Ccdc88c	82.65	0.267135288	0
P13439	Uridine 5'-monophosphate synthase	Umps	98.96	0.269820072	0
A0JP43	EF-hand calcium-binding domain-containing protein 5	Efcab5	132.72	0.280831627	0
P58389	Serine/threonine-protein phosphatase 2A activator	Ptpa	24.17	0.283654029	0.01
Q9JJA7	Cyclin-L2 OS=Mus musculus	Ccnl2	64.77	0.286504797	0
Q65Z40	Wings apart-like protein homolog	Wapl	93.96	0.286504797	0.03
Q3USH5	Splicing factor, suppressor of white-apricot homolog	Sfswap	18.44	0.289384215	0

E9PY46	Intraflagellar transport protein 140 homolog	Ift140	60.44	0.298197268	0
Q8BI84	Transport and Golgi organization protein 1 homolog	Mia3	79.39	0.304221247	0
Q3UJV1	Coiled-coil domain-containing protein 61	Ccdc61	62.76	0.310366955	0.05
Q8VCE9	Pleckstrin homology domain-containing family H member 3	Plekhh3	41.21	0.319819026	0.01
Q402B2	WD repeat-containing protein 93	Wdr93	26.84	0.323033258	0.03
Q9DC22	DDB1- and CUL4-associated factor 6	Dcaf6	43.22	0.326279793	0
P0DM40	Fer-1-like protein 5	Fer1l5	64.41	0.329558956	0
Q80VW7	AT-hook-containing transcription factor	Akna	120.31	0.329558956	0.01
Q9CQ76	Nephrocan OS=Mus musculus	Nepn	62.73	0.339595511	0
Q8C7R4	Ubiquitin-like modifier-activating enzyme 6	Uba6	70.72	0.34645583	0.02
Q9D9T8	EF-hand domain-containing protein	Efhc1	41.5	0.357006971	0
P35761	Dual specificity protein kinase TTK	Ttk	55.54	0.360594947	0.04
Q69ZT1	Fanconi-associated nuclease 1	Fan1	58.77	0.367879441	0
O55123	Stromelysin-2	Mmp10	74.49	0.367879441	0
Q9D3S3	Sorting nexin-29	Snx29	90.72	0.375311092	0
Q8VC12	Urocanate hydratase	Uroc1	17.94	0.379083027	0.03
P35436	Glutamate receptor ionotropic,	Grin2a	47.15	0.382892894	0.06
Q68SN8	Fc receptor-like protein 5	Fcrl5	36.2	0.386741028	0.01
Q61313	Transcription factor AP-2-beta	Tfap2b	265.96	0.394553708	0.06
O89032	SH3 and PX domain-containing protein 2A	Sh3pxd2a	63.67	0.394553708	0.02
O88444	Adenylate cyclase type 1	Adcy1	29.94	0.402524213	0.02
Q6URW6	Myosin-14	Myh14	36.99	0.406569669	0.02
Q69ZX6	MORC family CW-type zinc finger protein 2A	Morc2a	36.84	0.406569669	0.02
Q91YR5	Methyltransferase-like protein 13	Mettl13	70.63	0.406569669	0.06
P21784	V(D)J recombination-activating protein 2	Rag2	12.72	0.414782914	0.02

Q68FF0	Uncharacterized protein KIAA1841	Kiaa1841	184.57	0.414782914	0.02
O88573	AF4/FMR2 family member 1	Aff1	98.58	0.418951547	0.03
P97484	Leukocyte immunoglobulin-like receptor subfamily B member 3	Lilrb3	79.83	0.427414922	0.09
Q1HKZ5	Mitogen-activated protein kinase kinase kinase 13	Map3k13	96.18	0.427414922	0.04
Q80TH2	Erbin	Erbin	41.69	0.431710535	0.06
Q03391	Glutamate receptor ionotropic, NMDA 2D	Grin2d	79.79	0.436049294	0.03
A2RSJ4	UHRF1-binding protein 1-like	Uhrf1bp1l	73.99	0.440431658	0.09
Q6PGG2	GEM-interacting protein	Gmip	20.89	0.444858065	0.01
Q8CHB8	Tubulin polyglutamylase TTLL5	Ttll5	44.92	0.444858065	0.01
Q6ZPR6	Inhibitor of Bruton tyrosine kinase	Ibtk	52.85	0.453844786	0.1
Q8BLR5	PH and SEC7 domain-containing protein 4	Psd4	69.96	0.453844786	0.07
Q8BRC6	Cilia- and flagella-associated protein 91	Maats1	58.96	0.463013077	0.06
Q9QUQ5	Short transient receptor potential channel 4	Trpc4	4.32	0.463013077	0.21
Q9R1B9	Slit homolog 2 protein	Slit2	93.96	0.467666431	0.19
Q61739	Integrin alpha-6	Itga6	56.04	0.467666431	0.01
Q9JIM3	DNA excision repair protein ERCC-6-like 2	Ercc6l2	126.09	0.477113911	0
P97868	E3 ubiquitin-protein ligase RBBP6	Rbbp6	123.07	0.477113911	0
Q64521	Glycerol-3-phosphate dehydrogenase, mitochondrial	Gpd2	34.65	0.481908981	0.01
O35595	Protein patched homolog 2	Ptch2	47.13	0.481908981	0.15
C0LLJ0	Importin subunit alpha-8	Kpna7	156.9	0.486752242	0
Q9Z1N9	Protein unc-13 homolog B	Unc13b	78.66	0.491644208	0.02
Q8VDR9	Dedicator of cytokinesis protein 6	Dock6	57.98	0.491644208	0.03
Q91WJ8	Far upstream element-binding protein 1	Fubp1	148.29	0.491644208	0.24
Q6V3W6	Dynein regulatory complex subunit 7	Drc7	45.09	0.49658531	0.03
Q80TI1	Pleckstrin homology domain-containing family H member 1	Plekhh1	22.44	0.49658531	0.04

D3Z3C6	AN1-type zinc finger protein 4	Zfand4	34.17	0.49658531	0.04
Q62252	Sperm surface protein Sp17	Spa17	10.47	0.49658531	0.09
P31750	RAC-alpha serine/threonine-protein kinase	Akt1	53.76	0.50157607	0.03
Q8BL66	Early endosome antigen 1	Eea1	34.06	0.50157607	0.01
Q76MZ3	Serine/threonine-protein phosphatase 2A 65 kDa regulatory subunit A alpha isoform	Ppp2r1a	106.4	0.516851321	0.15
P53762	Aryl hydrocarbon receptor nuclear translocator	Arnt	16.58	0.522045789	0.16
Q05D44	Eukaryotic translation initiation factor 5B	Eif5b	20.03	0.527292432	0

Table 1B: list of up-regulated protein in control vs. PD group.

Accession	Description	Gene	Score	Fold change	P values
Q3US17	Zinc finger protein 48	Znf48	53.45	2.033991215	0.94
Q9DBV3	Probable ATP-dependent RNA helicase DHX34	Dhx34	26.81	2.054433269	0.84
Q69ZH9	Rho GTPase-activating protein 23	Arhgap23	85.29	2.075080647	0.99
Q6PCM1	Lysine-specific demethylase 3A	Kdm3a	73.5	2.075080647	0.1
Q61410	cGMP-dependent protein kinase 2	Prkg2	48.47	2.095935534	0.99
Q78PY7	Staphylococcal nuclease domain-containing protein 1	Snd1	49.95	2.095935534	0.93
Q61712	DnaJ homolog subfamily C member 1	Dnajc1	179.33	2.095935534	0.98
O08644	Ephrin type-B receptor 6	Ephb6	57.2	2.117000017	0.82
Q2TV84	Transient receptor potential cation channel subfamily M member 1	Trpm1	70.19	2.117000017	0.99
Q9DBT3	Coiled-coil domain-containing protein 97	Ccdc97	163.38	2.117000017	0.96
Q3UYK3	TBC1 domain family member 9 OS=Mus musculus OX=10090 GN= PE=2 SV=2	Tbc1d9	34.44	2.1382762	0.82
Q8BXZ1	Protein disulfide-isomerase TMX3	Tmx3	78.36	2.1382762	0.85
Q60520	Paired amphipathic helix protein Sin3a	Sin3a	56.89	2.159766213	0.91
A2AVR2	Maestro heat-like repeat-containing protein family member 7	Mroh7	44.46	2.203396474	1
Q3U821	WD repeat-containing protein 75	Wdr75	56.32	2.203396474	0.75
O35253	Mothers against decapentaplegic homolog 7	Smad7	124.06	2.247907992	0.76
Q8CIQ7	Dedicator of cytokinesis protein 3	Dock3	61.43	2.247907992	1
Q5IR70	Cancer-associated gene 1 protein homolog	Cage1	72.97	2.247907992	1
Q8VDG6	Mitogen-activated protein kinase kinase kinase 21	Map3k21	63.8	2.247907992	0.97
Q6P549	Phosphatidylinositol 3,4,5-trisphosphate 5-phosphatase 2	Inppl1	58.2	2.247907992	0.98
P55937	Golgin subfamily A member 3	Golga3	96.77	2.293318702	0.96

Q8R3N1	Nucleolar protein 14	Nop14	79.3	2.293318702	0.99
O88207	Collagen alpha-1(V) chain	Col5a1	59.36	2.316366916	0.93
Q9Z103	Activity-dependent neuroprotector homeobox protein	Adnp	89.03	2.316366916	1
Q91V83	TELO2-interacting protein 1 homolog	Tti1	15.61	2.339646908	0.98
Q80WJ6	Multidrug resistance-associated protein 9	Abcc12	13.84	2.339646908	0.99
Q8CGM1	Adhesion G protein-coupled receptor B2	Adgrb2	27.72	2.339646908	1
Q9WTP5	Cadherin-22	Cdh22	14.61	2.363160728	0.97
Q09M02	Cytosolic carboxypeptidase-like protein 5	Agbl5	67.6	2.363160728	1
Q8C262	Interferon-inducible GTPase 5	Irgc	52.61	2.386910865	0.82
Q8R5C8	Zinc finger MYND domain-containing protein 11	Zmynd11	38.62	2.410899695	0.99
Q9Z280	Phospholipase D1	Pld1	41.71	2.459603053	0.98
O35134	DNA-directed RNA polymerase I subunit RPA1	Polr1a	66.4	2.559981412	0.97
P70298	Homeobox protein cut-like 2	Cux2	52.91	2.559981412	0.81
Q02788	Collagen alpha-2(VI) chain	Col6a2	122.36	2.585709628	1
B9EJ80	PDZ domain-containing protein 8	Pdzd8	125.57	2.637944535	0.92
Q9Z315	U4/U6.U5 tri-snRNP-associated protein 1	Sart1	89.04	2.637944535	0.92
Q3UHX0	Nucleolar protein 8	Nol8	36.16	2.745600989	0.95
Q922B9	Sperm-specific antigen 2 homolog	Ssfa2	38.63	2.773194711	1
O88393	Transforming growth factor beta receptor type 3	Tgfbr3	40.02	2.857650982	0.96
Q60592	Microtubule-associated serine/threonine-protein kinase 2	Mast2	49.97	2.944679677	0.99
Q69Z38	Pseudopodium-enriched atypical kinase 1	Peak1	55.29	2.944679677	1
Q0VF58	Collagen alpha-1(XIX) chain	Col19a1	44.36	3.034358438	0.95
Q8K368	Fanconi anemia group I protein homolog	Fanci	29.85	3.064854218	0.97
Q6P5D4	Centrosomal protein of 135 kDa	Cep135	58.95	3.064854218	1

Q9R0L6	Pericentriolar material 1 protein	Pcm1	72.96	3.064854218	0.78
Q8BZ81	Leucine-rich repeat transmembrane neuronal protein 3	Lrrtm3	4.51	3.095656485	0.96
Q4QY64	ATPase family AAA domain-containing protein 5	Atad5	45.34	3.158192834	0.99
Q60767	Lymphocyte antigen 75	Ly75	76.17	3.158192834	0.97
Q6PFQ7	Ras GTPase-activating protein 4	Rasa4	50.73	3.2219925	1
Q8CJ19	[F-actin]-monooxygenase MICAL3	Mical3	92.55	3.287081395	1
Q8R2Q4	Ribosome-releasing factor 2, mitochondrial	Gfm2	145.38	3.287081395	0.95
Q6PDH0	Pleckstrin homology-like domain family B member 1	Phldb1	48.26	3.35348478	1
Q9D2Y5	Sorting nexin-20	Snx20	125.27	3.455613498	0.96
Q8K1M6	Dynamin-1-like protein	Dnm1	93.75	3.525421454	0.98
Q8K4G5	Actin-binding LIM protein 1	Ablim1	138.74	3.525421454	1
Q3TZ89	Protein transport protein Sec31B	Sec31b	26.71	3.669296493	1
Q9R020	Zinc finger Ran-binding domain-containing protein	Zranb2	71.65	3.743421574	1
Q8R3K3	Pentatricopeptide repeat-containing protein 2, mitochondrial	Ptcd2	133.7	3.78104355	1
Q8JZX4	Splicing factor 45	Rbm17	191.31	3.857425623	0.96
Q80YR2	Protein FAM160B2	Fam16	82.59	3.896193358	1
P18608	Non-histone chromosomal protein HMG-14	Hmgn1	63.86	4.05519987	1
Q80Z10	Astrotactin-2	Astn2	113.17	4.095955267	1
Q69ZZ6	Transmembrane and coiled-coil domains protein 1	Tmcc1	105.42	4.095955267	0.99
Q9D8M4	60S ribosomal protein L7-like 1	Rpl7l1	98.5	4.137120263	1
Q64455	Receptor-type tyrosine-protein phosphatase eta	Ptprj	82.44	4.178698973	1
Q9CZH8	Coiled-coil domain-containing protein 77	Ccdc77	68.39	4.220696059	1
P19426	Negative elongation factor E OS=Mus musculus OX=10090 GN= PE=1 SV=2	Nelfe	233.74	4.220696059	1
Q8BYR2	Serine/threonine-protein kinase LATS1	Lats1	82.67	4.392945765	1

O35227	Disintegrin and metalloproteinase domain-containing protein 7	Adam7	84.53	4.572225108	0.99
Q8K1K4	Centromere protein I	Cenpi	32.05	4.61817669	0.1
Q6ZQK0	Condensin-2 complex subunit D3	Ncapd3	19.64	4.61817669	0.89
Q8R516	E3 ubiquitin-protein ligase MIB2	Mib2	97.88	4.61817669	0.97
Q62190	Macrophage-stimulating protein receptor	Mst1r	36.56	4.711469958	1
Q5PRF0	HEAT repeat-containing protein 5A	Heatr5a	173.88	4.953032542	1
Q04592	Proprotein convertase subtilisin/kexin type 5	Pcsk5	118.56	5.053090341	1
Q3UWM4	Lysine-specific demethylase 7A	Kdm7a	117.3	5.419481015	1
A2ARA8	Integrin alpha-8	Itga8	111.53	5.528961689	0.99
Q80TK0	Uncharacterized protein KIAA1107	Kiaa1107	56.56	5.697343477	0.99
Q8BTT6	Digestive organ expansion factor homolog	Diexf	22.27	6.423736863	1
Q80TQ2	Ubiquitin carboxyl-terminal hydrolase CYLD	Cyld	128.62	7.242743123	0.45
O89114	DnaJ homolog subfamily B member 5	Dnajb5	104.76	7.242743123	1
Q8K1N2	Pleckstrin homology-like domain family B member 2	Phldb2	148.05	7.924822589	0.95
Q9DBM2	Peroxisomal bifunctional enzyme	Ehhadh	22.72	8.935213626	1
Q8CFE4	SCY1-like protein 2	Scyl2	20.66	11.02317743	1
Q8BWZ3	N-alpha-acetyltransferase 25, NatB auxiliary subunit	Naa25	34.99	11.24586017	1
Q8VCC9	Spondin-1	Spon1	14.42	12.06127624	0.99
Q8BH53	Cilia- and flagella-associated protein 69	Cfap69	40.4	13.06582357	1
Q99MV7	RING finger protein 17	Rnf17	80.2	15.48698524	1
Q9D6A1	Unconventional myosin-Ih	Myo1h	25.15	16.94545953	1
Q62234	Myomesin-1	Myom1	79.57	18.1741471	1
Q9EPR5	VPS10 domain-containing receptor SorCS2	Sorcs2	136.48	18.91584739	1
Q569L8	Centromere protein J	Cenpj	29.79	20.697232	1

P97369	Neutrophil cytosol factor 4	Ncf4	43.81	23.33606681	1
P23116	Eukaryotic translation initiation factor 3 subunit A	Eif3a	79.2	24.77908717	1
Q9JLG8	Calpain-15	Capn15	38.93	28.50273093	1
Q9D4K7	Coiled-coil domain-containing protein 105	Ccdc105	24.52	29.37077447	0.99
Q8BMA5	Protein NPAT	Npat	66.01	38.47466972	0.99
Q9QY42	Prosaposin receptor GPR37	Gpr37	191.96	57.39746799	0.23
Q60610	T-lymphoma invasion and metastasis-inducing protein 1	Tiam1	170.78	126.469371	0.2
Q99PP7	E3 ubiquitin-protein ligase TRIM33	Trim33	92.95	139.7702576	1
Q8K352	SAM and SH3 domain-containing protein 3	Sash3	41.94	639.0610809	1

Table 2A: list of down-regulated protein in PD vs. Treatment group.

Accession	Description	Gene	Score	Fold change	P values
Q8K440	ATP-binding cassette sub-family A member 8-B	Abca8b	4.22	0.069948	0
P97369	Neutrophil cytosol factor 4	Ncf4	49.82	0.132655	0
Q6PFX7	Neuronal tyrosine-phosphorylated phosphoinositide-3-kinase adapter 1	Nyap1	4.91	0.163654	0
P13864	DNA (cytosine-5)-methyltransferase 1	Dnmt1	44.99	0.214381	0
Q8R1Q0	Syntaxin-19	Stx19	26.01	0.261846	0.01
Q8R5C8	Zinc finger MYND domain-containing protein 11	Zmynd11	20.04	0.275271	0
Q8K1K4	Centromere protein I	Cenpi	22.85	0.440432	0.03
Q8BZQ7	Anaphase-promoting complex subunit 2	Anapc2	20.56	0.467666	0
Q8BZ05	Arf-GAP with Rho-GAP domain, ANK repeat and PH domain-containing protein 2	Arap2	25.48	0.491644	0
P31750	RAC-alpha serine/threonine-protein kinase	Akt1	63.32	0.511709	0.14
Q6PCM1	Lysine-specific demethylase 3A	Kdm3a	14.41	0.52722	0.14
O35253	Mothers against decapentaplegic homolog 7	Smad7	39.84	0.55988	0
Q6P549	Phosphatidylinositol 3,4,5-trisphosphate 5-phosphatase 2	Inppl1	15.62	0.56555	0.03
Q9Z280	Phospholipase D1	Pld1	45.45	0.606531	0.2
Q8R2Q4	Ribosome-releasing factor 2, mitochondrial	Gfm2	24.03	0.612626	0.01
Q60610	T-lymphoma invasion and metastasis-inducing protein 1	Tiam1	31.11	0.650509	0.07
Q80TQ2	Ubiquitin carboxyl-terminal hydrolase CYLD	Cyld	16.8	0.657047	0.03
Q9QY42	Prosaposin receptor GPR37	Gpr37	10.31	0.66365	0.07
Q64455	Receptor-type tyrosine-protein phosphatase eta	Ptprj	7.7	0.66365	0.01

Table 2B: list of up-regulated protein in PD vs. treatment group.

Accession	Description	Gene	Score	Fold change	P values
P31750	RAC-alpha serine/threonine-protein kinase	Akt1	63.32	1.877611	0.81
P40630	Transcription factor A, mitochondrial	Tfam	93.78	1.879013	1
Q3UH60	Disco-interacting protein 2 homolog B	Dip2b	33.8	2.013753	0.92
Q9DAZ9	Abscission/NoCut checkpoint regulator	Zfyve19	173.52	2.159766	0.96
Q80T11	Usher syndrome type-1G protein homolog	Ush1g	17.67	2.4109	0.98
P53762	Aryl hydrocarbon receptor nuclear translocator	Arnt	16.58	2.43513	0.91
Q76MZ3	Serine/threonine-protein phosphatase 2A 65 kDa regulatory subunit A alpha isoform	Ppp2r1a	10.16	2.534509	0.93
Q8BL66	Early endosome antigen 1	Eea1	34.06	3.095656	0.86
Q6PFQ7	Ras GTPase-activating protein 4	Rasa4	30.1	3.221993	1
Q6P9K8	Caskin-1	Caskin1	11.12	3.287081	1
P70208	Plexin-A3	Plxna3	13.23	3.59664	1
P70670	Nascent polypeptide-associated complex subunit alpha, muscle-specific form	Naca	31.4	7.690609	1
Q5SXJ3	Fanconi anemia group J protein homolog	Brip1	22.12	9.874937	0.07
Q05D44	Eukaryotic translation initiation factor 5B	Eif5b	20.03	11.24586	0.08
Q9QUQ5	Short transient receptor potential channel 4	Trpc4	7.04	1.822119	1
P35436	Glutamate receptor ionotropic, NMDA 2A	Grin2a	9	1.584074	1

Table 3: Enriched Pathway analysis. The gene sets indicates the pathway id in wikipathway. Description represents the name of the pathways in which the DEPs were reported. Size indicates the total number of proteins in each pathway. FDR (false discovery rate), for dark blue colour FDR <0.05 and for light blue colour FDR >0.05. Enrichment ratio is the ratio of the obsereved count over expected count by chance.

Gene Set	Description	Size	Expect	Ratio	P Value	FDR
WP3673	Hfe effect on hepcidin production	7	0.0076	131.57	0.007581	1
WP1263	Mitochondrial Gene Expression	19	0.02063	48.474	0.020469	1
WP1246	Hypothetical Network for Drug Addiction	31	0.033659	29.71	0.033223	1
WP3638	Parkinsons Disease Pathway	39	0.042345	23.615	0.041652	1
WP113	TGF Beta Signaling Pathway	52	0.05646	17.712	0.055223	1
WP3632	Lung fibrosis	61	0.066232	15.098	0.064528	1
WP2075	Alzheimers Disease	75	0.081433	12.28	0.078857	1
WP339	ESC Pluripotency Pathways	118	0.12812	7.8051	0.12177	1
WP1397	Odorant GPCRs	189	0.20521	4.873	0.18912	1
WP2292	Chemokine signaling pathway	190	0.2063	4.8474	0.19004	1

Figures

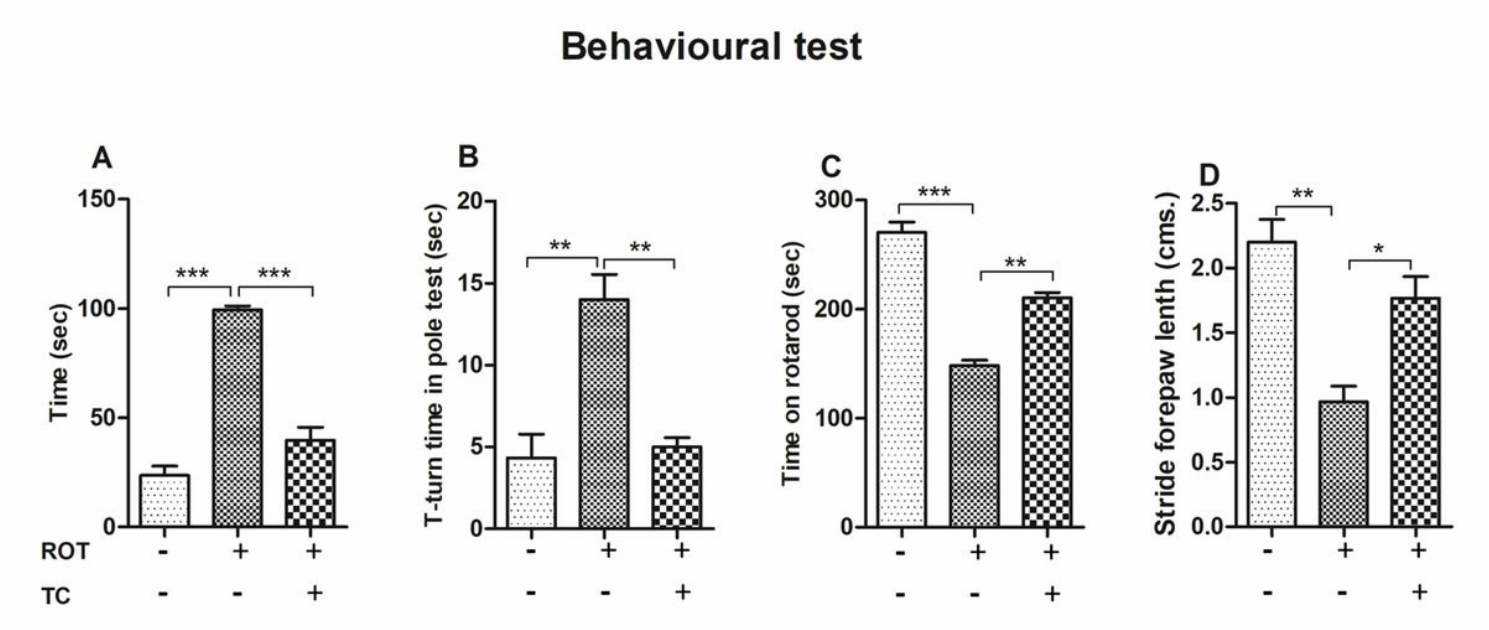

Figure 1

Neurobehavioral test of ROT- intoxicated mice treated with Tc. (A) Time in Cataleptic test (B) T-turn time in the pole test (C) Time on the rotarod test (D) Stride forepaw length in Foot print test. Values are represented in the form of mean ± SEM (n = 8). ∗p < 0.05, ∗∗p < 0.01, and ∗∗∗p < 0.001.

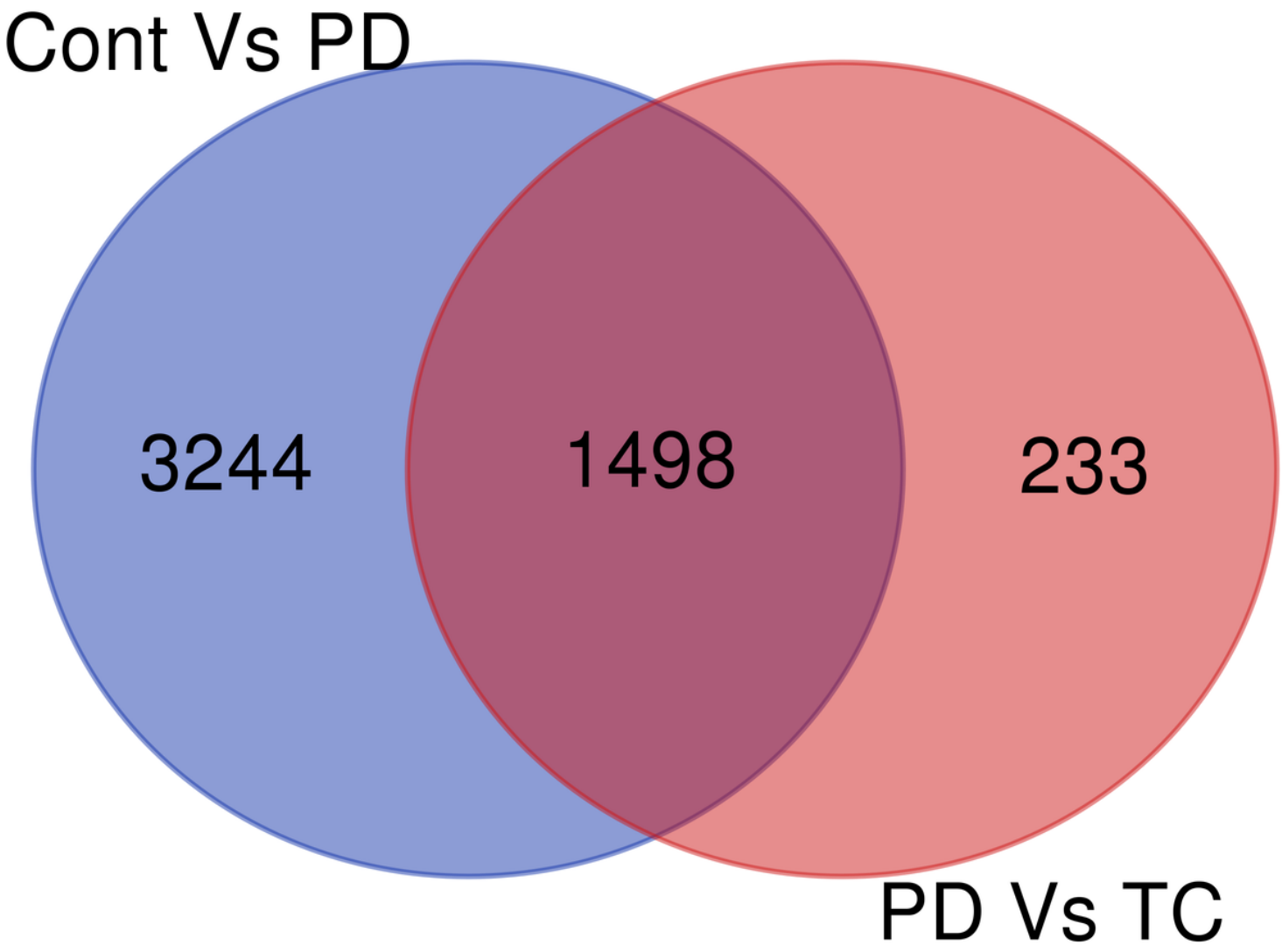

Figure 2

Venn diagram reprsenting the unique and common proteins between control vs PD and PD vs Tc groups.

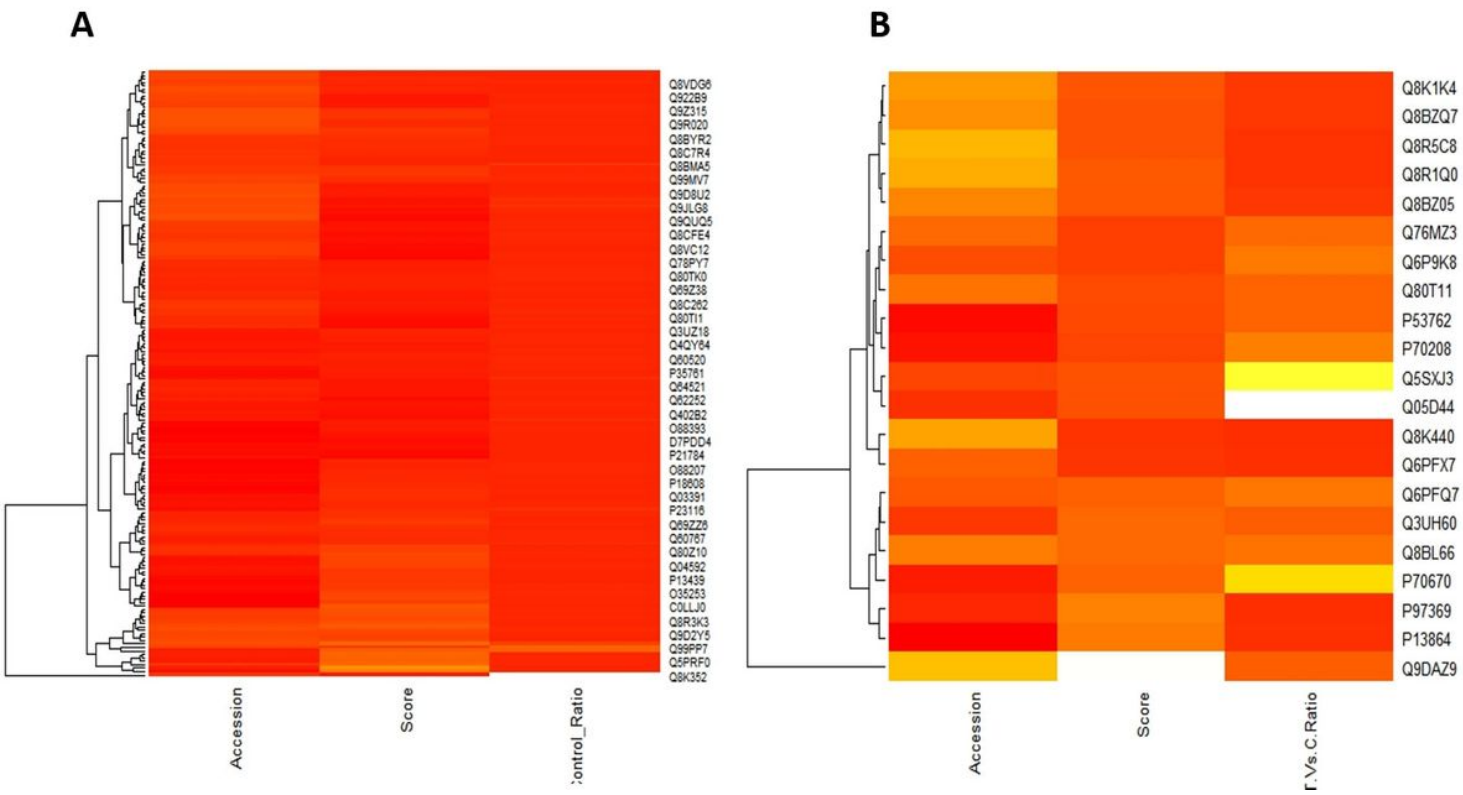

Figure 3

Heat Map representing the expression levels of the diffrentially expressed proteins. The red coloured regions indicate a high level of protein expression, the orange regions represent the mid value of the protein expression and the yellow regions indicates a low expression of the proteins. Samples are clustered on the basis of relative expression, accession number and p-value.

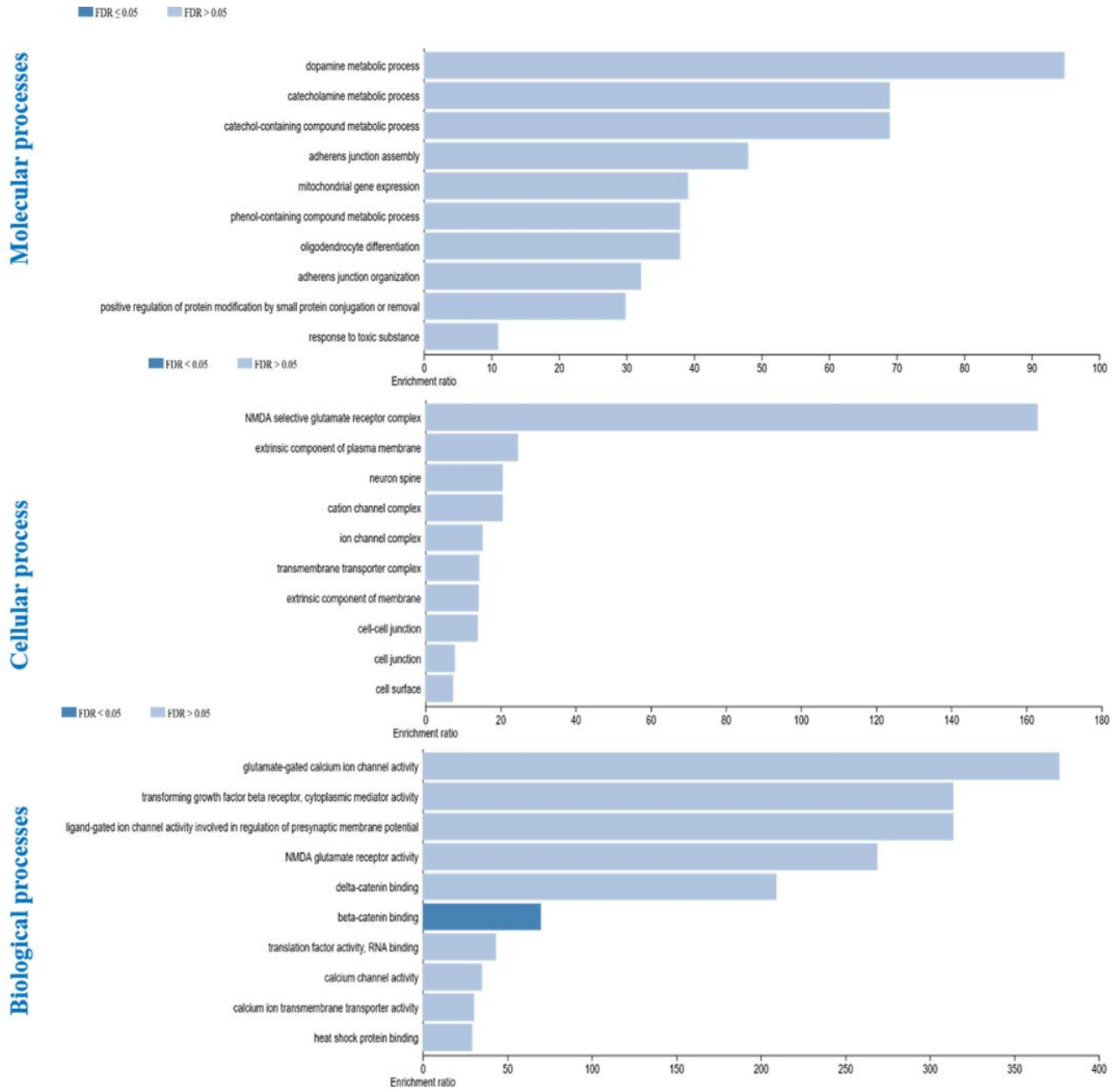

Figure 4

Gene Ontology Enrichment Analysis of the DEPs.

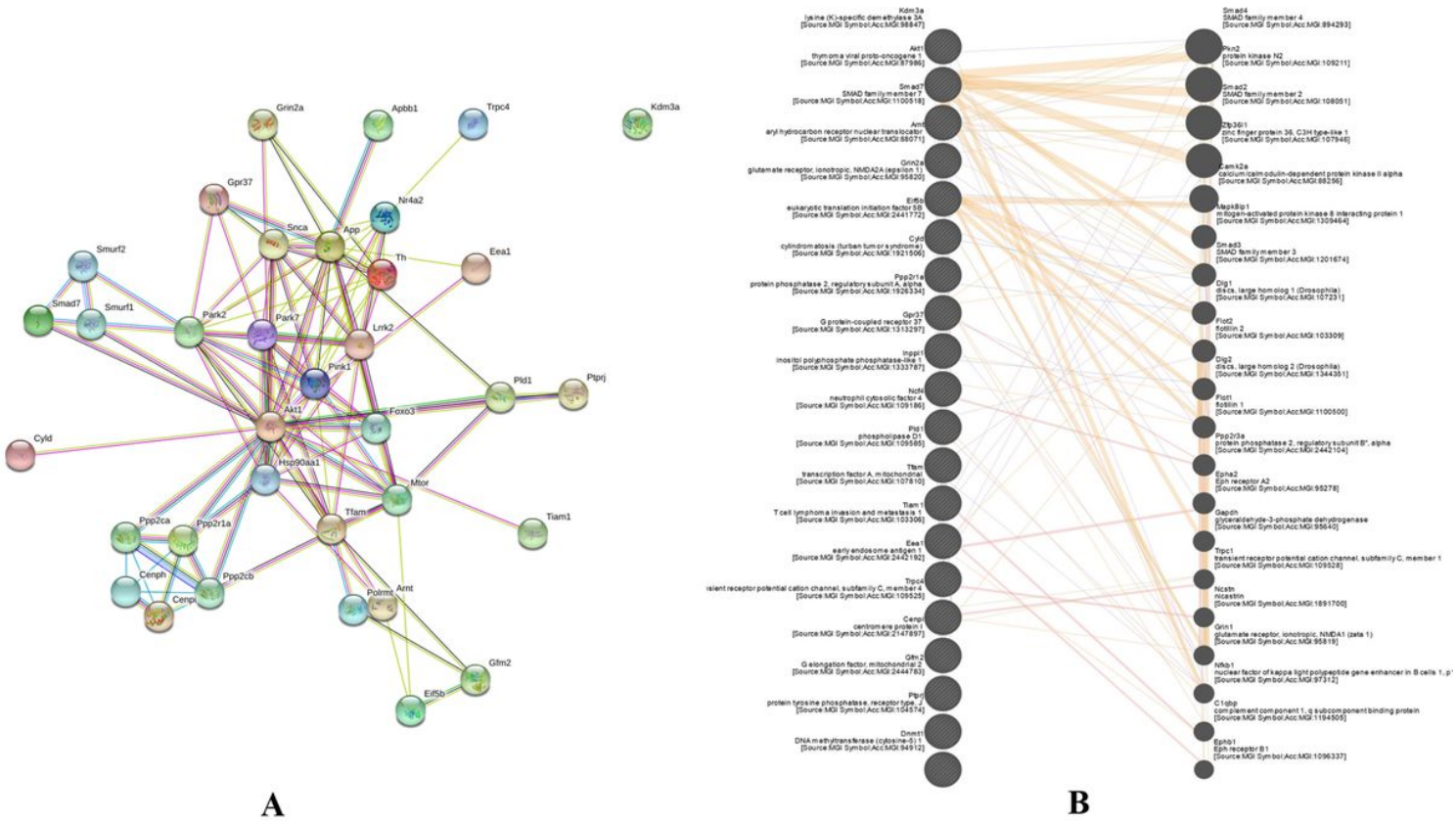

Figure 5

Protein-Protein interaction network among the DEPs, along with gene-gene interaction network. (A) PPI network was constructed using String. (B) In gene-gene interaction the nodes with lines on them were the proteins obtained in the results whereas the nodes without lines on them were the proteins from the database (Analysis performed by Genemania). In both these networks the different coloured edges indicates the different interactions among the DEPs. The width of the edge reprents the strength of the intractions between the DEPs and predicted proteins.

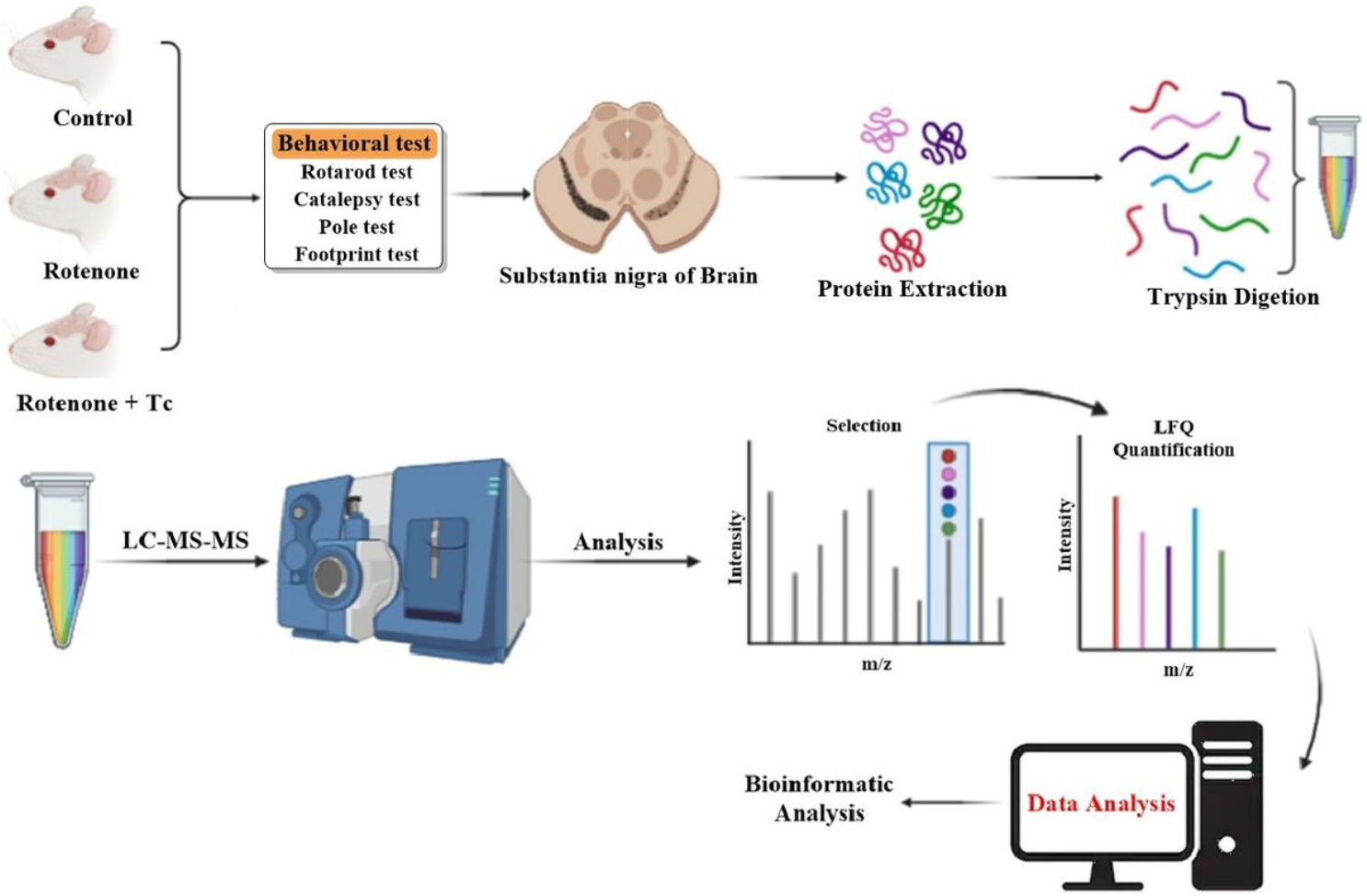

Figure 6

Graphical representation of methodology used for LFQ analysis of Control, PD and treatment groups. Proteins were isolate and digested with multiple proteases followed by LC-MS/MS. Each sample were processed in triplicate.

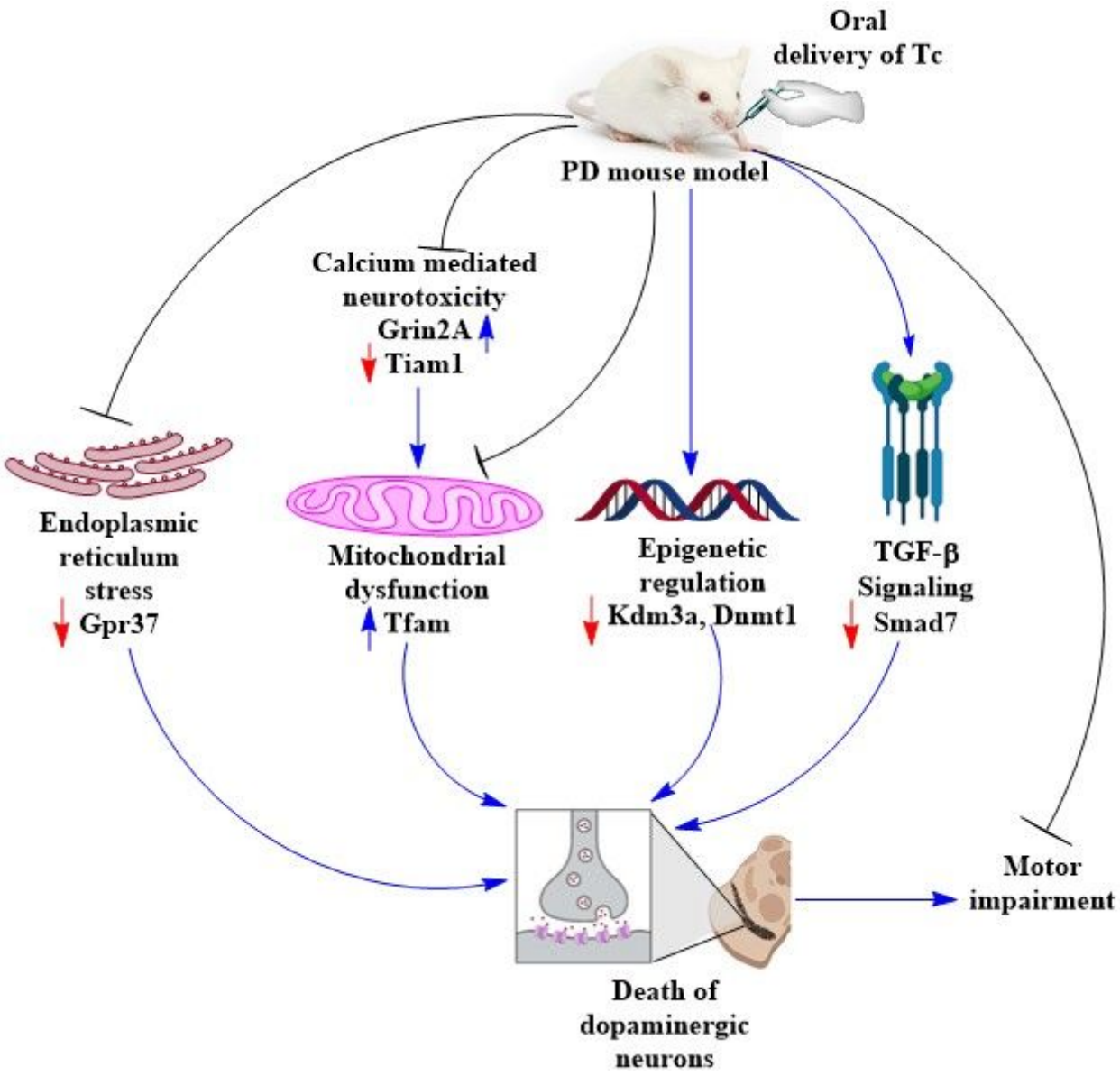

Figure 7

Representative model of biochemical pathways modulated by Tc treatment in Parkinsonian mice.

Supplementary Files

This is a list of supplementary files associated with this preprint. Click to download.

- Supplimentryfile1.xlsx
- supplimentryfile2.docx